Title: Have human impacts exceeded climate in shaping mammalian distributions?

Running title: mammalian distributions

Authors: Xin Chen[1], Luis José Aguirre-López[2], Xiao Feng[2*]

Affiliations:
[1]Appalachian Laboratory, University of Maryland Center for Environmental Science, Frostburg, MD 21532, USA;
[2]Department of Biology, University of North Carolina, Chapel Hill, NC 27599, USA;
[*]Corresponding author: Email: fengxiao.sci@gmail.com

Abstract
Human impacts are increasingly recognized as drivers of biogeographic patterns, yet it remains unclear whether they surpass climate in shaping species distributions. Here we aim to investigate the relative importance of anthropogenic vs. climatic factors in determining mammalian distributions. We modeled the relationship between the geographic distributions of 219 mammal species and 12 representative anthropogenic and climatic factors, and quantified variable importance with ecological niche models and explainable artificial intelligence at range-wide and local scales. We also constructed the response curve of human impact index (HII) for each species, and investigated the association between the response curves and species' biological traits. We found that anthropogenic factors were ranked as top contributors for nearly half of the species examined, and the average effect of HII has exceeded that of average and seasonal climatic conditions across spatial scales. While dominating effects of HII were widespread across the continent, the other factors often showed spatial clusters at different subsections of species' ranges. Species' response to human impacts displayed diverse patterns, and the positive responses were associated with traits of reduced conflicts with humans, faster reproduction, and greater mobility. The extent of human impacts is comparable to, and in some cases exceeds, that of climate in shaping contemporary mammalian biogeography patterns. The heterogeneous responses of mammal species to human impacts highlight the need to broadly consider anthropogenic factors, in addition to climate, in studying biodiversity in the Anthropocene.

Introduction

Understanding the factors that shape species' geographic distributions is a central goal in ecology and biogeography (Lomolino *et al.* 2010; Relyea & Ricklefs 2013). Traditionally, large-scale distribution and biodiversity patterns have been attributed primarily to abiotic environmental gradients, especially climate, which forms the foundation of many biogeographic theories (Andrewartha & Birch 1954; MacArthur 1984). However, this climate-centric view increasingly fails to capture the full reality of biodiversity dynamics in the Anthropocene, where human influence is both widespread and intensifying (Feng *et al.* 2024; Frans & Liu 2024; Helmus *et al.* 2014).

Human impacts are increasingly acknowledged as important drivers of species distributions (Burton *et al.* 2024; Kays *et al.* 2024; Suraci *et al.* 2021). For instance, the global human footprint has been shown to profoundly influence both native (Kays *et al.* 2024; Suraci *et al.* 2021) and invasive (Andrewartha & Birch 1954; MacArthur 1984) terrestrial mammal distributions. Higher road density is linked to reduced dispersal and increased habitat fragmentation, which restricts species ranges (Bennett 2017; Forman *et al.* 2003). Agricultural expansion negatively affects many mammals via habitat loss, although opportunistic species may benefit from new food resources (Gallego-Zamorano *et al.* 2020). Also, nighttime light and higher human population densities can disrupt mammal activity patterns (Gaynor *et al.* 2018).

There is no doubt that anthropogenic factors profoundly alter biogeographic patterns, but do their effects surpass those of climate? This distinction is critical for theoretical and practical reasons, as natural environmental factors, especially climate, are considered the major driver in many biogeographic, ecological, and evolutionary theories (Andrewartha & Birch 1954; MacArthur 1984), and many biodiversity conservation strategies are centered on climate change and less on the direct impact of humans (Caro *et al.* 2022; Chapman *et al.* 2014). If anthropogenic factors are comparable to or exceed climate in influencing species distributions, then we will face a new norm of thinking that anthropogenic and climatic factors shall always be considered together in ecological and biogeographic research and biodiversity conservation (Feng *et al.* 2024).

An increasing number of studies have investigated the importance of anthropogenic and climatic drivers, as well as their interactions, in influencing biogeography and biodiversity patterns. For example, Gallardo et al. found human-related variables (e.g., distance to ports) to be the primary drivers for range expansion of ~17–25% of nonnative species (Gallardo et al. 2015; Gallardo & Aldridge 2013). In contrast, Kays et al. (2024) found human population density to be less important than climate in predicting native mammal abundance (Kays et al. 2024). Other studies have evaluated the joint influence of anthropogenic and climatic factors on species' geographic distributions (Jiang et al. 2023; Li et al. 2025); for instance, Jiang et al. (2023) found that climate variables contributed more than human disturbance variables to the longitudinal and latitudinal changes in 19 Qinghai–Tibet Plateau vertebrates (Jiang et al. 2023). Previous literature also identified the importance of the interaction between climate change and land conversion in influencing population abundances, community composition, and biodiversity patterns (Montràs-Janer et al. 2024; Williams and Newbold 2021). However, previous investigations often report only range-wide variable importance and overlook its spatial variation, even though spatially explicit information (e.g., variable importance for a given location) is critical for guiding conservation actions at local and regional scales (Franklin et al. 2014; Waldock et al. 2024).

Hence, a comprehensive, quantitative assessment comparing anthropogenic and climatic drivers across different spatial scales is critical.

To fill this gap, we performed a systematic modeling experiment to investigate the effects of anthropogenic and climatic factors in determining the geographic distributions of 219 mammal species across North America. The study area is enriched with wide coverage of species distribution and environmental data, comprising gradients of anthropogenic and climatic conditions. We considered six anthropogenic factors to represent different types of human effects (Feng *et al.* 2024), and six climatic factors to represent mean and seasonal climatic conditions that are widely recognized for their effects in determining species' geographic distributions (Lomolino *et al.* 2010) (Table S2). We also leveraged the technique of explainable artificial intelligence (xAI) (Barredo Arrieta *et al.* 2020) to map the spatially explicit influence of both anthropogenic and climatic factors on species distributions. We further quantified the variation of species' responses to HII, a synthetic variable that stood out as the top contributing anthropogenic factor, and investigated their associations with a set of biological traits. We hypothesized that i) anthropogenic factors have exceeded the importance of climate in shaping contemporary mammalian distributions across spatial scales, and ii) the associations between species distribution and anthropogenic factors are related to species traits.

Material and methods

Occurrence data

Our study focused on mammal species whose geographic ranges are mainly (> 70%) in North America, where large amounts of species observational records have been collected (Feng *et al.* 2022; Hughes *et al.* 2021). We used this criterion (see *Supplementary Methods*) to identify species that have abundant observation data across their ranges, thus making more robust inferences on the relationship between species distribution and climatic or anthropogenic factors. We downloaded the presence records of these species from the Global Biodiversity Information Facility (GBIF) database (GBIF.org 2023). We filtered the presence records based on the basis of records and only kept records coded as preserved specimen, human observation, occurrence, material citation, machine observation, and material sample (see the treatment and sensitivity analysis of sampling bias below). We retained the presence records that were collected between 1990 and 2020 to represent the more recent distribution of the focal species; this temporal extent was also aligned with that of the environmental variables to be used in the ecological niche model (Feng *et al.* 2019b). We excluded the presences that were outside of slightly enlarged IUCN range maps (buffered by 1/10 of the radius of a range map assuming its circular shape) to avoid potential vagrant records. The buffered IUCN range was subsequently used as the modeling domain for each species. We applied spatial thinning to the occurrence data and only kept one occurrence in each 10 km grid to minimize the impact of sampling bias (Boria *et al.* 2014). We further excluded species with fewer than 50 spatially unique presence records to ensure more robust model performance. We also excluded species that have relatively low model evaluation metrics. Following the criteria discussed above, we retained a list of 219 species (Table S1, Fig. S1) for investigating the influence of climatic and anthropogenic factors on their distributions.

Bioclimatic and anthropogenic factors

For the ecological models, we selected six out of 19 bioclimatic variables that are commonly used in ecological niche modeling literature, and selected 6 out of 25 representative anthropogenic factors that may potentially affect species' geographic distributions compiled in (Feng *et al.* 2024). The six bioclimatic factors were annual mean temperature (Annual mean T), annual precipitation (Annual P), mean temperature of warmest/coldest quarter (Maximum/Minimum T), and precipitation of wettest/driest quarter (Wettest/Driest P) (Table S2). These variables represent the mean and seasonal climatic conditions that are widely recognized for their effects in determining species' geographic distributions (Lomolino *et al.* 2010). We calculated these bioclimatic variables based on monthly climatic data between 1990-2020 at 1 km resolution from AdaptWest database (AdaptWest Project 2022).

The six representative anthropogenic factors were human impact index (HII), highway density, cropland percentage (Cropland), pasture percentage (Pasture), nighttime lights, and human population (Table S2). We also avoided high correlation [correlation coefficient $|r| < 0.7$, Fig. S2; (Dormann *et al.* 2013; Feng *et al.* 2019a)] among them and better matching their temporal extents (2010-2018) to those of species' occurrence and climatic data. These variables have been found to influence mammalian distributions from regional to global scales (Burton *et al.* 2024; Cheeseman *et al.* 2024; Guarnieri *et al.* 2024; Tucker *et al.* 2021). Please see more detailed justifications of each variable in *Supplementary Methods*. The selected variables encompassed a wide spectrum of human impacts, allowing a more comprehensive comparison of human impacts against those of climate in shaping present mammalian distributions across North America. All environmental layers were aligned with North America at 1 km spatial resolution.

Modeling

We performed ecological niche models using the Maxent algorithm (version 3.4.3). Maxent effectively handles presence-background data and has demonstrated consistently high accuracy in modeling a variety of species distributions (Elith *et al.* 2006; Phillips & Dudík 2008). We included linear and quadratic features to avoid overly complex response functions to ensure ecologically relevant interpretation of the relationship between species' geographic distribution and environmental predictors (Merow *et al.* 2013). The default regularization parameters of Maxent were used. To account for sampling bias that may occur in the occurrence data (e.g., research-grade data from iNaturalist that are part of the GBIF download), we generated target group background data with the same underlying bias as the occurrence data for each species (Phillips *et al.* 2009). The selection of 10,000 target group background points was weighted by the sampling bias surface of occurrences obtained through kernel density estimation (Fitzpatrick *et al.* 2013). The sampling bias surface was restricted within the modeling domain (i.e., buffered IUCN range) for each species. We performed five-fold cross-validation by partitioning occurrence data of each species into training (80%) and test (20%) datasets and evaluated model performance using the area under the receiver operating characteristic curve (AUC) and the continuous Boyce index (CBI) (see more details in *Supplementary Methods*). Besides using target group background data, we performed an additional sensitivity analysis to evaluate the impact of potential sampling bias in the model outcomes; we repeated the modeling experiment by excluding all human observations (mostly data from iNaturalist) and obtained largely consistent results (Figs. S3 & S10).

We used permutation importance of each variable to represent its contribution to the ecological niche model. The permutation importance of a variable is the amount of decrease in training AUC when the values of a focal variable were permuted. Larger values of permutation importance indicate greater variable importance in modeling the relationship between the probability of presence and environmental conditions. The permutation importance is typically normalized to percentages, running from 0 to 100% (Phillips 2005). Here we used permutation importance to compare the relative contribution of anthropogenic factors versus bioclimatic factors. Note that the modeling approach used here is generally considered correlative (compared with mechanistic approaches) (Peterson et al. 2015); thus, the permutation importance does not necessarily indicate the strength of any underlying biological mechanism. The influence of collinearity on the permutation importance was expected to be minimal, as the predictors included were not highly correlated (Strobl *et al.* 2007) (Fig. S2). In addition, we also calculated the rank of variable contribution, ranging from 1, meaning most important, to 12, meaning least important.

We performed two additional experiments to evaluate the robustness of the modeling results toward the choice of modeling algorithm (using boosted regression tree, or BRT; Fig. S4) and variable collinearity (using principal component analysis of 19 bioclimatic variables; Fig. S5). We selected the first six principal components (PCs) that together account for 97.7% of the variation (Fig. S21). Compared to the previously selected temperature or precipitation factors, each of the selected PCs represented both temperature and precipitation factors. Please see more details in *Supplementary Methods*.

Response to human impacts in environmental and geographic space

In our preliminary analysis, HII stood out to be highly important for most mammal species. Therefore, we further investigated the response curve of HII for each species. The response curve represents the predicted relative probability of presence of a species given a gradient of an environmental variable, which is HII in this case. To compare the response curve of all species, the response curve was projected to the range of HII values available in North America using the 'enmSdmX' package (Smith et al. 2023). We note that model extrapolation was involved when constructing the response curves, though we considered the risk to be relatively low. The breadth of HII values used in model training was relatively wide. The mean minimum and maximum HII values of all species investigated were 0.05 (sd=0.51) and 5024.79 (sd=438.70), respectively, which are very close to the range of HII in the study area (0-5865; Fig. S13). Also, we only included linear and quadratic features during model training to avoid overly complex response functions; thus, we expect the selected strategy to be less prone to extrapolation risk compared with more complex response curves (Chen et al. 2024).

We categorized the response curves into five groups (I, II, III, IV, V), reflecting the different levels of HII where the relative probability of presence for a species reaches the highest value. More specifically, we derived one response index for each curve. The response index considered the proportion of segments with positive slopes and the position where the predicted relative probability of presence peaked. Each response curve was evenly separated into 5865 segments (5865 is the maximum value of HII in the study area). The index will reach a maximum value of 3 when a monotonically increasing response curve peaks at the top-right corner (i.e., relative probability of presence = 1 and HII = 5865). Based on the response indices, we performed a

cluster analysis using k-means based on the 'stats' package in R. The number of groups (i.e., five) was determined using the 'factoextra' package, which explored different numbers of groups (k); there was a sharp decline of within-cluster sums of squares from k = 1 to k = 4, followed by a smaller reduction after k = 5, indicating that five clusters provide a reasonable explanation for variation in response-curve structure and avoid over-partitioning (Fig. S14). The trends in each group are analogous to similar concepts used in the literature (Berman et al. 2024; Tryjanowski et al. 2020): Group I is comparable to urban avoiders (or human-sensitive species), and their probability of presences is negatively associated with human impacts; Groups II, III, and IV are comparable to urban adapters (or intermediate species) whose probability of presences increases along with human impact, but only up to a particular threshold; Group V is more like urban exploiters (or human-associated species) whose probability of presences is largely positively associated with human impacts.

We also generated SHapley Additive exPlanations (SHAP) (Lundberg & Lee 2017; Shapley 1953) maps to show species' response to environmental factors across the geographic space. SHAP is one of the explainable artificial intelligence (xAI) tools that provides an interpretation of the covariate effect on the predicted outcome at the observation level (here, a grid cell). A SHAP value indicates the difference between what a variable contributes to a prediction in each location, and what the variable is expected to contribute given the mean model prediction. Compared with permutation importance, a SHAP value represents a predictor's contribution to the prediction for that specific grid cell, i.e., the location-specific effect of each predictor (Waldock *et al.* 2024). A SHAP value of 0 suggests no contribution, while a deviation from 0 indicates a larger positive or negative contribution. We calculated SHAP values for each of the 12 variables used in the main modeling experiment across the modeling domain of a focal species using the R package 'itsdm' with 100 times of simulations (Song & Estes 2023). For every species, there would be 12 layers of SHAP maps, each representing a variable. We aggregated the SHAP maps for each variable and each mammal order to illustrate the overall importance of a focal variable. The aggregation was performed at 40-km spatial resolution to facilitate the visual comparison across groups. We also identified cases where a focal variable has the highest absolute SHAP value at a focal pixel (among SHAP values of all 12 variables at the same pixel); this was performed for each pixel across each species' geographic range and aggregated across different mammal orders or all species.

Traits data

To further investigate whether species' response to HII was affected by their biological traits, we compiled a set of mammal traits from the COMBINE database (Soria *et al.* 2021). Overall, we selected the trait data that are known to be strong predictors of mammals' response to human impacts and that are available for the 219 species (Table S4). We avoided trait variables that were highly correlated. The 15 selected traits include: 1) body mass, 2) female sexual maturity, 3) gestation length, 4) litter size, 5) number of litters, 6) weaning age, 7) generation length, 8) hibernation or torpor, 9) diet breadth, 10) habitat breadth, 11) trophic level, 12) foraging strata, 13) fossoriality, 14) activity cycle, and 15) volant capacity. Please see more detailed justifications of the selected traits in *Supplementary Methods*.

Statistical analyses

We conducted linear regressions using ordinary least squares (OLS) to investigate the relationship between species' responses to HII and species traits. We used the cumulative sum of the relative probability of presence along the response curve of HII as the response variable and 15 biological traits (6 categorical and 9 numerical) as candidate predictors (Table S4). The adult body mass was log transformed to minimize the difference between extreme large and small values. All the numerical variables were scaled to have a mean of zero and standard deviation of one for easier comparison among their corresponding regression coefficients derived from the OLS models. With all species (n=219), we performed a stepwise model selection based on the Akaike information criterion (AIC) to obtain the models with the lowest AIC. In addition, we built stepwise models using OLS for each mammal order to investigate potential differences among their responses to HII; in this case, a predictor would be excluded from a model if all species in that order have the same values for the variable (i.e., no variation present among species). Orders lacking sufficient sample size to allow at least two residual degrees of freedom were not modeled individually, though they remained in the all-species model. The OLS models involved cross-species comparisons, and the biological traits could exhibit phylogenetic signal and affect the interpretation of models. Therefore, we tested the residuals of the stepwise-selected models for phylogenetic signal (Revell 2010). We estimated Pagel's λ for the model residuals across 1,000 phylogenetic trees obtained from PHYLACINE 1.2.1 (Faurby et al. 2018; Faurby et al. 2020) using the 'phytools' R package (Revell 2024). As we found no significant phylogenetic signal (lambda $\approx$ 0; Table S5), we only presented the results of the OLS model.

Results

Anthropogenic vs. climatic factors

The test AUC and CBI of the Maxent models were 0.72±0.06 and 0.82±0.14, suggesting good model performance. Overall, HII and mean temperature of the coldest and warmest quarter (Minimum/Maximum T) stood out to be the top three contributing predictors among all predictors; the mean permutation importance was 30.5 (sd = 23.0), 13.3 (sd = 11.9), and 10.4 (sd = 12.7) for HII, Minimum T, and Maximum T, respectively (Fig. 1). Similar patterns were also found in the modeling results by using non-human observations, BRT, or PCA (Figs. S10-S12). The permutation importance of HII and its rank were significantly greater than those of Minimum/Maximum T and annual T/P across all species (Fig. 1A, Wilcoxon signed-rank test, $p < 0.001$) and many of the orders considered (Figs. S6-9). Similar pattern was found when comparing permutation importance at the species level: HII had greater permutation importance than the top contributing climatic variables (Minimum/Maximum T and annual T/P) for a large number and fraction of species (Table S3).

Anthropogenic factors were ranked as the top contributor for 52.5% (115 of 219) of the cases considered (Fig. 2). The percentage varied slightly in the sensitivity analyses: the percentage was 45.4% when human observations were excluded from model training, 59.8% when BRT algorithm was used for model training, and 62.1% when raw climatic factors were replaced with principal components (Figs. S3-S5).

HII stood out as the top contributor for 45.2% of the species considered (99 of 219; Fig. 2A). This pattern was more pronounced for Chiroptera (67.9%; 19 of 28), Artiodactyla (62.5%; 5 of 8), and Carnivora (61.1%; 11 of 18), than for Lagomorpha (53.8%; 7 of 13), Rodentia (50.4%; 64 of 127), and Soricomorpha (33.3%; 8 of 24) (Fig. 2B).

Following HII and Minimum/Maximum T, the highly influencing variables were percentages of Cropland and Pasture among anthropogenic factors and annual mean temperature (Annual mean T) and annual precipitation (Annual P) among climatic factors (Fig. 2A). In such cases, Cropland was ranked as the top contributing variable for 13 species, and Pasture for 3 species; these species were mainly in Rodentia, Chiroptera, and Carnivora orders. Annual mean T and Annual P were ranked as top contributing variables for 39 species.

Effects of anthropogenic factors

Overall, the response curves for HII were more dynamic after 2,000 units (Fig. 3F). The varied response curves were classified into five groups (I-V) (Fig. 3). The greatest percentage of V (71.4%; 20 of 28) was found for the Chiroptera order. In contrast, most species of Group I were found in the Rodentia order (7.9%; 10 of 127), followed by the Soricomorpha (4.2%; 1 of 24) and Chiroptera (3.6%; 1 of 28) orders. Despite the species exhibiting contrasting responses to HII between V and I, we also identified a large number of species with unimodal response curves (mainly in II and III), and a small number of species showing nearly flat response curves (Fig. 3).

Species in Group IV had the largest range sizes, while range size generally increased from Group I to Group IV (Fig. S15). Although species in Group V had the highest predicted probability of presence at high HII, their range sizes were smaller than those of Group IV. The differences in sample size (occurrences) among the five groups were very similar to those of the range size (Fig. S18). Regarding geographic patterns, we found that species in Group I were more concentrated in Mexico and the Southeastern US (Fig. S17); Groups II and III had wider geographic distributions, with the highest richness in western North America; and Groups IV and V also had wider geographic distributions, with the highest richness in eastern and central North America (Fig. S17).

The aggregated SHAP maps showed that the HII had the most spatially extensive signal across North America compared with the other anthropogenic or climatic factors (Figs. 4, 5, S19, S20). HII effects were predominantly negative across the study area, with scattered areas of positive effects (Fig. 4). Cropland effects were concentrated mainly in the Midwest and Great Plains (Fig. 5) and were generally negative (Fig. 4). Pasture effects were also mostly negative (Fig. 4), with the strongest signals concentrated west of the Great Plains (Fig. 5). Overall, the spatial patterns in the SHAP maps of the anthropogenic factors were similar across different orders (Fig. 4). The signal of climatic variables was less pronounced in aggregated SHAP maps compared to that of HII (Figs. 4, 5, S19, S20); among the climatic variables, the signal of temperature-related variables was more pronounced than that of precipitation-related variables. The positive and negative effects of temperature-related variables were spatially separated: the negative effect of cold temperature (temperature of the coldest quarter) was concentrated in the northern part of North America, and the positive effect was concentrated in the southern part; the pattern was generally reversed for annual mean temperature and warm temperature (temperature of the warmest quarter) (Fig. 4).

Biological traits and species response to HII

We found five biological traits significantly related to species' response (summed slope of response curve) to HII when considering all species together (Fig. 6). Among the five traits, the

three numerical traits were adult mass (0.18, $p < 0.001$), gestation length (-0.11, $p < 0.001$) and generation length (-0.08, $p < 0.05$), while for the ordinal traits, volant species showed a significantly positive response compared to non-volant species (0.60, $p < 0.001$); and a negative response for ground foraging compared to aerial foraging (-0.44, $p < 0.05$). Adult mass had significant positive effects for Lagomorpha and Soricomorpha, and a marginal negative effect for Carnivora (-0.18, $p = 0.057$). For Rodentia and Chiroptera, adult mass was not selected. The full list of estimated coefficients and their associated p-values are shown in Table S6.

Among the six traits of growth and reproduction strategies, gestation length and litters per year had significant negative effects for Soricomorpha (-1.99 and -0.69, $p < 0$ .05), while litter size showed a positive response (0.29, $p < 0.05$). For Rodentia, weaning age had significant positive effects (0.25, $p < 0.001$). For Chiroptera, weaning age, female maturity, and litter size showed positive but not significant effects.

When assessing species' activities vertically, volant terrestrial mammals showed positive association with HII compared with non-volant species. For the volant mammals (e.g., Chiroptera), diet breadth showed significantly negative effects (-0.18, $p < 0.05$). Above-ground dwelling had a significant negative effect for Rodentia (-0.21, $p < 0.01$) compared with ground dwelling. When assessing species' activities temporally, mixed activity patterns (nocturnal/crepuscular/diurnal) showed negative effects, compared with nocturnal-only for Soricomorpha (-1.23, $p < 0.05$).

Discussion

Anthropogenic vs. climatic factors

We performed a systematic modeling experiment to investigate the effects of anthropogenic and climatic factors in determining the geographic distributions of 219 mammal species across North America. We found that anthropogenic factors were comparable to, and in some cases exceeded, climatic factors in shaping the contemporary (1990-2020) distributions for these mammal species. The range-wide permutation importances of anthropogenic factors were ranked as top contributors for more than half (52.5%; 115 of 219) of the North American mammals investigated (Fig. 2). In particular, range-wide permutation importance of HII exceeded that of both average and seasonal climatic conditions when averaged across species, and for a large fraction of orders and species considered (Figs. 1, S6-S9, Table S3). These patterns are robust to the choice of occurrence data (Fig. S10), modeling algorithm (Fig. S11), and predictor collinearity (Fig. S12).

The range-wide permutation importances were also reflected by the SHAP analysis of variable importance at pixel levels. The aggregated SHAP maps showed that, while no single predictor played a dominant role across the whole continent (i.e., every pixel), HII had the most spatially extensive signal across North America, suggesting that its importance was not restricted to a few highly modified regions (Figs. 4-5). The SHAP maps of HII were predominantly negative with scattered areas of positive effects. The widespread negative SHAP values are likely caused by the negative effect of mid-high HII values on the probability of presence of many species (Fig. 3A-C), and scattered positive effects are likely related to the relatively fewer species whose probability of presence is positively associated with high HII values, and the areas with extremely high HII are spatially limited (Fig. 3E, S1, S16). In contrast, the effects of cropland

and pasture were more geographically concentrated, mostly in places where such land use is of high intensity. The positive and negative effects of temperature-related variables are often spatially separated, suggesting that temperature is likely acting as the limiting factor at the northern and southern boundaries of species' geographic distributions.

Variable importance has been recognized to be scale-dependent in the literature of ecological niche modeling or species distribution modeling (Smith and Santos 2020). Our study was performed at both range scale (range-wide permutation importances) and pixel scale (pixel-wise SHAP values). The broad agreement between the two approaches supported the importance of anthropogenic predictors across scales. Future studies could extend this framework to intermediate scales (e.g., ecoregions, protected areas, or county boundaries), or to finer spatial grains using microclimate and high-resolution anthropogenic data, or to a scale at which species respond to the environments (Smith and Santos 2020).

The temporal dimension of the variable importance should also be noted. Climate has shaped mammalian biogeography over deep historical timescales and forms the foundation of many biogeographic theories (Andrewartha & Birch 1954; MacArthur 1984); in contrast, many anthropogenic pressures have intensified relatively recently in the "Anthropocene" (Lewis and Maslin 2015). Thus, our finding that anthropogenic predictors were comparable to, and in some cases more important than, climatic predictors should be interpreted as evidence that human impacts are strongly associated with present-day (1990-2020) mammal distributions. Future studies could further explore the changes of relative importance of anthropogenic and climatic factors through time. Our conclusion was different from (Kays *et al.* 2024); despite the differences in the methodology, the different conclusions could lie in the use of human predictors. We have considered more human predictors in our study, including a synthetic index that incorporates multiple dimensions of human impacts. Also, the camera trap data used in (Kays *et al.* 2024) might be slightly biased toward more natural areas, as the goal of camera traps is usually to observe wildlife in natural settings (Suraci *et al.* 2021).

HII was found to be the most determinant factor among the anthropogenic factors assessed. HII is a synthetic index that represents multiple dimensions of human impacts. Areas with high HII could either represent a high value of individual human effects or a high combined sum; thus, HII will likely have higher spatial heterogeneity than other individual anthropogenic or climatic factors. The synthetic nature of HII could potentially mask the importance of other anthropogenic factors and inflate its permutation importance. If so, the comparison of permutation importance between HII and individual climatic factors (temperature or precipitation) may be unfair; however, when comparing permutation importance of HII with PCs of 19 bioclimatic variables (while each PC represented both temperature and precipitation factors; Fig. S21), HII still commonly stood out as a top contributing variable (Fig. S12). Nevertheless, given the permutation importance found here, HII can potentially be used broadly in studying global change biology under human impacts, especially when the underlying human-related drivers on biological responses are unknown.

The dominant effects of anthropogenic factors support the claim that they should be treated as additional dimensions of the ecological niche "hypervolume" (Feng *et al.* 2024). Besides the ones analyzed here, many other anthropogenic variables are available at broad spatial and

temporal extents (Feng *et al.* 2024; Frans & Liu 2024), which makes them easily usable in biogeographic and ecological studies, biodiversity conservation, and beyond. The challenge is that these factors blur the classic abiotic–biotic distinction: human-generated conditions (e.g., heat islands, pollution, noise, and light) resemble abiotic factors, while human-provided resources (e.g., food, water) function as biotic subsidies. Thus, additional theoretical guidelines are needed.

The multifaceted responses to human impacts

Species' response curves to HII displayed diverse patterns with monotonic increases or decreases, parabolic shapes, or flat trends (Fig. 3). Our findings of the positive and negative associations between probability of species presences and human impacts are comparable to the scenarios of range expansions and contractions in terrestrial mammals since the 1970s (Pacifici *et al.* 2020). Given the projected increase of human impacts (Steffen *et al.* 2015), we may expect that there will not be uniform impacts on species distributions, but rather homogenization of fauna and decreased beta diversity in the future. The homogenization of biodiversity was known to be caused by the spread of non-native species (Aulus-Giacosa *et al.* 2024; Capinha *et al.* 2015); however, our study suggests that the homogenization of biodiversity could happen within the native fauna, by increasing the geographic distribution of species that are positively associated with human impacts and decreasing the ones that are not.

We also found more monotonic increases (n = 52) to human impacts than monotonic decreases (n = 7) (Fig. 3). One possible explanation is that the species assessed here were the "survivors" of historical impacts (Pineda-Munoz *et al.* 2021) (e.g., the megafauna extinction (Sandom *et al.* 2014)); thus, the species distribution data (between 1990 and 2020) and their spatial patterns could be the results of human impacts (Pineda-Munoz *et al.* 2021). Similarly, Finn et al. (2023) found the highest number of mammal species with increasing populations in North America and relatively fewer species with decreasing populations, despite more "losers" than "winners" at global scale (Finn *et al.* 2023).

In contrast with monotonic increases or decreases, we found a high proportion of parabolic-shaped response curves to HII (Fig. 3), suggesting many species could coexist with human pressure to a certain extent (Larson *et al.* 2020). However, the built environment in urban centers (e.g., parking lots) could be non-habitable for many species, and wild animals can suffer great human disturbance and mortality risk, e.g., because of noise and traffic (Soga & Gaston 2020; Suraci *et al.* 2021).

Biological traits and species' response to human impacts

We found that species more positively associated with human impacts shared traits of larger body mass (except for Carnivora), shorter gestation length, and flying capacity. These traits could potentially reduce the conflicts with humans, reflect faster reproduction, and enhance mobility to explore new habitats and avoid disturbances.

Body mass is a broadly recognized biological trait that is related to many other biological traits and macroecology patterns (Smith & Lyons 2011). Similarly, we found body mass to be a significant predictor for the response of species' probability of presence to human impact. Interestingly, a smaller adult mass was selected for Carnivora; they are commonly recognized as

predators in food webs and can compete for food and space with humans (Treves & Karanth 2003). Such conflicts lead to higher extinction risk for large-bodied predators (Sandom et al. 2014). Medium-sized carnivores, such as raccoons and skunks, can adapt well to anthropogenically modified landscapes by exploiting food sources and shelters in urban environments, achieving high population densities (Bateman & Fleming 2012). Their potential conflicts with humans may explain that half of the carnivores investigated showed a unimodal response curve, while their probability of presence decreases at high HII (Fig. 3C & 3G). As an opposite example, rodents grow larger as human population density increases, likely because of the increase in quality and abundance of rodent food sources (Pergams & Lawler 2009). Bats were found to have increased morphological traits, such as forearm length, a standard general index of body size in bats (Kunz 1974), as responses to Anthropogenic environmental change (Yue *et al.* 2019).

Omnivory provides flexibility for species' food resources, and here omnivory was found to be positively associated with the presence of North American soricomorphs under human impacts. Indeed, with the expansion of human population and settlement, humans have distributed anthropogenic foods (e.g., trash, livestock, and crop) worldwide (Oro *et al.* 2013), which have been broadly used by omnivorous mammals (Fedriani *et al.* 2001). Similar patterns have been found in China, where the proportion of omnivores increased with human presence and modification of the landscape (Li *et al.* 2022). Besides mammals, the proliferation of omnivorous species in human-modified landscapes was also found in birds (Cristaldi *et al.* 2017) and fish (Neves *et al.* 2024). Despite the positive effect of omnivory, the use of anthropogenic foods can also be associated with high mortality rates in urban areas because of human-wildlife conflict or roadkill; thus, anthropogenic foods could become ecological traps (Grilo *et al.* 2020; Lamb *et al.* 2017). Interestingly, diet breadth was negatively associated with Chiroptera. It is possible that, in urban areas, bats have access to abundant resources, leading to a more homogeneous and specialized diet focused on high-quality, protein-rich animal sources (Guiry & Buckley 2018).

Shorter gestation length was found to be favored under human impacts. As opposed to slow development and fewer offspring, the strategy of faster reproduction has been selected for under human disturbance landscapes. This strategy is commonly associated with successful invaders that leverage opportunities to obtain propagule pressure to get established (Bielby *et al.* 2007; Sakai *et al.* 2001). Faster reproduction may help mammals to offset human-induced disturbances and mortalities (Santini *et al.* 2019; Suraci *et al.* 2021).

Volant capacity is also favored under human impacts. This is likely because non-volant mammals usually face increased mortality risks because of vehicle collisions, predation by domestic animals, or limited dispersal across anthropogenic matrices (de Andrade 2022; Corrêa *et al.* 2018). Volant capacity can enhance the mobility and dispersal of mammals, especially bats (Yalden & Morris 1975), and thus put volant mammals in an advantageous position under urban settings (Parkins & Clark 2015) or make them less or unaffected by urbanization (Richardson *et al.* 2021). Indeed, we found that Chiroptera (bats) had the highest fraction of species classified as Group V (Fig. 3), and their probability of presence was positively associated with HII.

Humans have also profoundly changed the temporal activity of wild animals. Mammals are known to become more nocturnal in order to avoid humans (Gaynor *et al.* 2018). We found that

carnivorous mammals with a wider temporal niche (mixed activity patterns) are more associated with higher human impacts. Conversely, mixed activity patterns are negatively associated with Socicomorpha when compared to nocturnal activity only. If species have a narrower temporal niche, it might result in increased intensity of competition and predation due to a larger overlap of temporal niches (Van Scoyoc *et al.* 2023), a dynamic that may especially affect carnivorous mammals. On the other hand, soricomorphs are predominantly nocturnal, and this lifestyle may act as a temporal refuge, benefiting them by minimizing overlap and avoiding conflict with diurnal human activities (Gaynor et al. 2018).

The mixed responses to human impacts and their associations with biological traits highlight new challenges of biodiversity conservation in the human-dominated era. Species may benefit from one factor (e.g., human food subsidies) but be harmed by another (e.g., traffic). Understanding species' tolerance to multiple anthropogenic factors will help guide mitigation, regulation, and conservation priorities (Burton *et al.* 2024; Howard *et al.* 2020; Venter *et al.* 2016). Current conservation strategies focus heavily on climate change, but our findings highlight the need to also incorporate anthropogenic drivers such as urbanization, population growth, agriculture/pasture, and pollution, which are increasingly available in future projections (Gao & O'Neill 2020; Li *et al.* 2021).

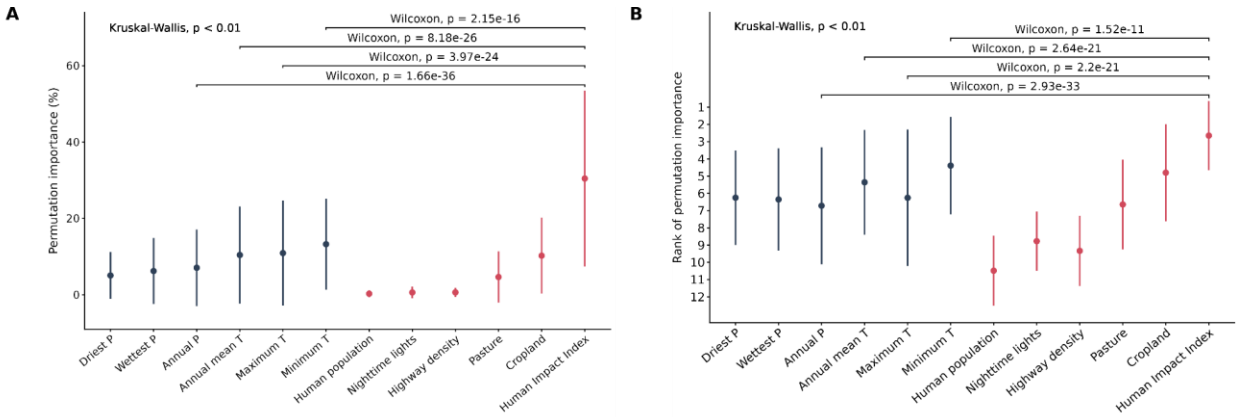

Figure 1. Variable importance for each predictor. Panel A shows the variable importance, and panel B shows the rank of variable importance for each predictor variable. Climatic variables are colored as blue, and anthropogenic factors are colored as red. The error bars represent the one SD around the means. The differences in variable importance and rank of variables were found using the Kruskal-Wallis test. The pairwise differences were performed between human impact index and the top four climatic variables, using the Wilcoxon signed-rank test (Wilcoxon) with a Hommel (Hommel 1988) correction for multiple hypothesis testing. The p-values < 0.01 and < 0.001 indicated significant differences.

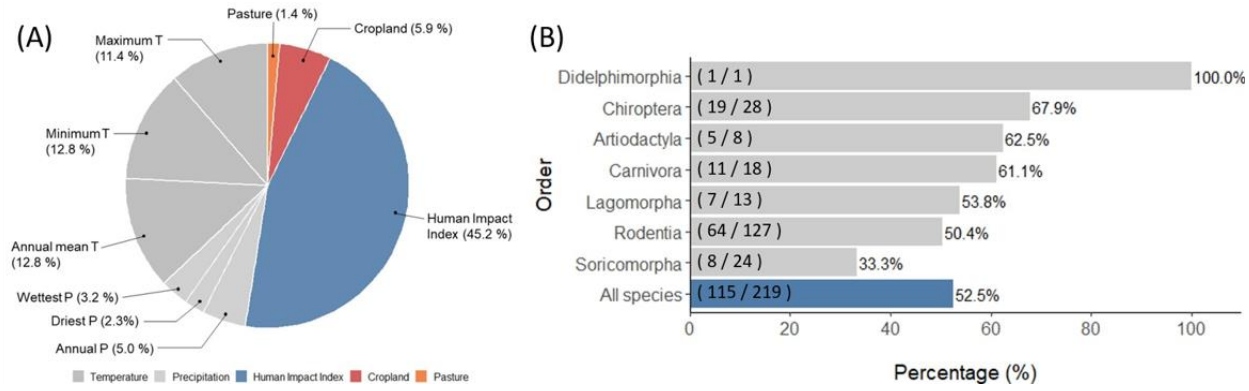

Figure 2. Overview of top contributing factors. Panel A shows the percentage of top contributing factors across all North American mammals (n = 219). Panel B shows the percentage of species within each mammal order that has an anthropogenic factor ranked as the top contributing factor.

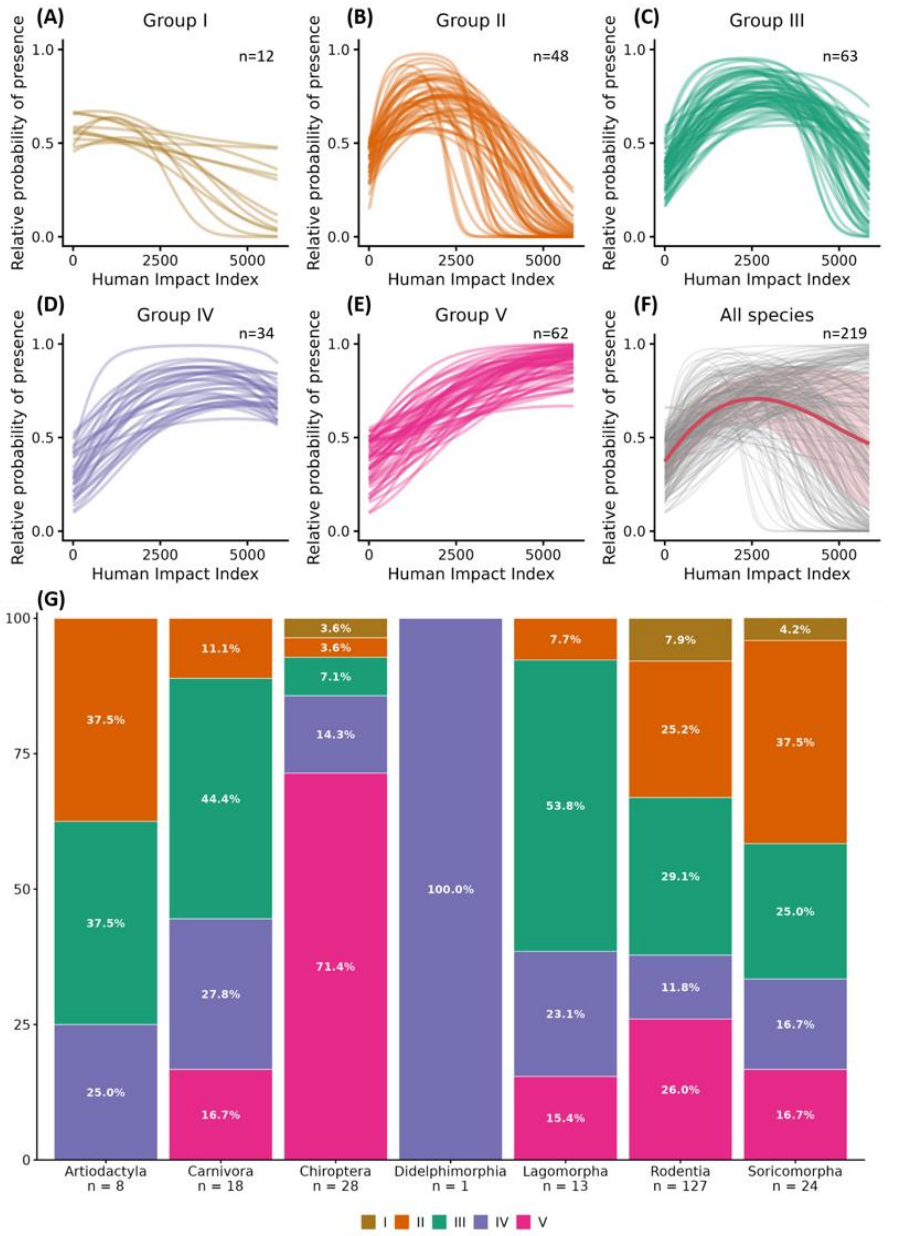

Figure 3. Grouping of mammals based on their responses to human impact index (HII). Panels A-F show response curves of 219 species, which are categorized into five groups (I, II, III, IV, V). The grouping reflects different levels of HII where the relative probability of presence for a species reaches the highest value (see Methods). Panel F shows the mean response (red line) across all species at each HII value; the red shaded band represents one standard deviation around the mean response, showing increased intraspecific variation with increased HII values. The x-axis of a response curve represents the magnitude of HII. For instance, a value of < 100 would represent the areas with little or no human impact (e.g., natural forests and wetlands), a value around 2500 would indicate a medium level of human impacts (e.g., suburbs of St. Louis, Vancouver, or Guadalajara), and values up to 5,000 would represent areas with high human impacts (e.g., metropolitan districts in New York City, Toronto, and Mexico City) (see Fig. S1). Panel G shows the percentages of species in each mammal order that are categorized in five groups (I-V).

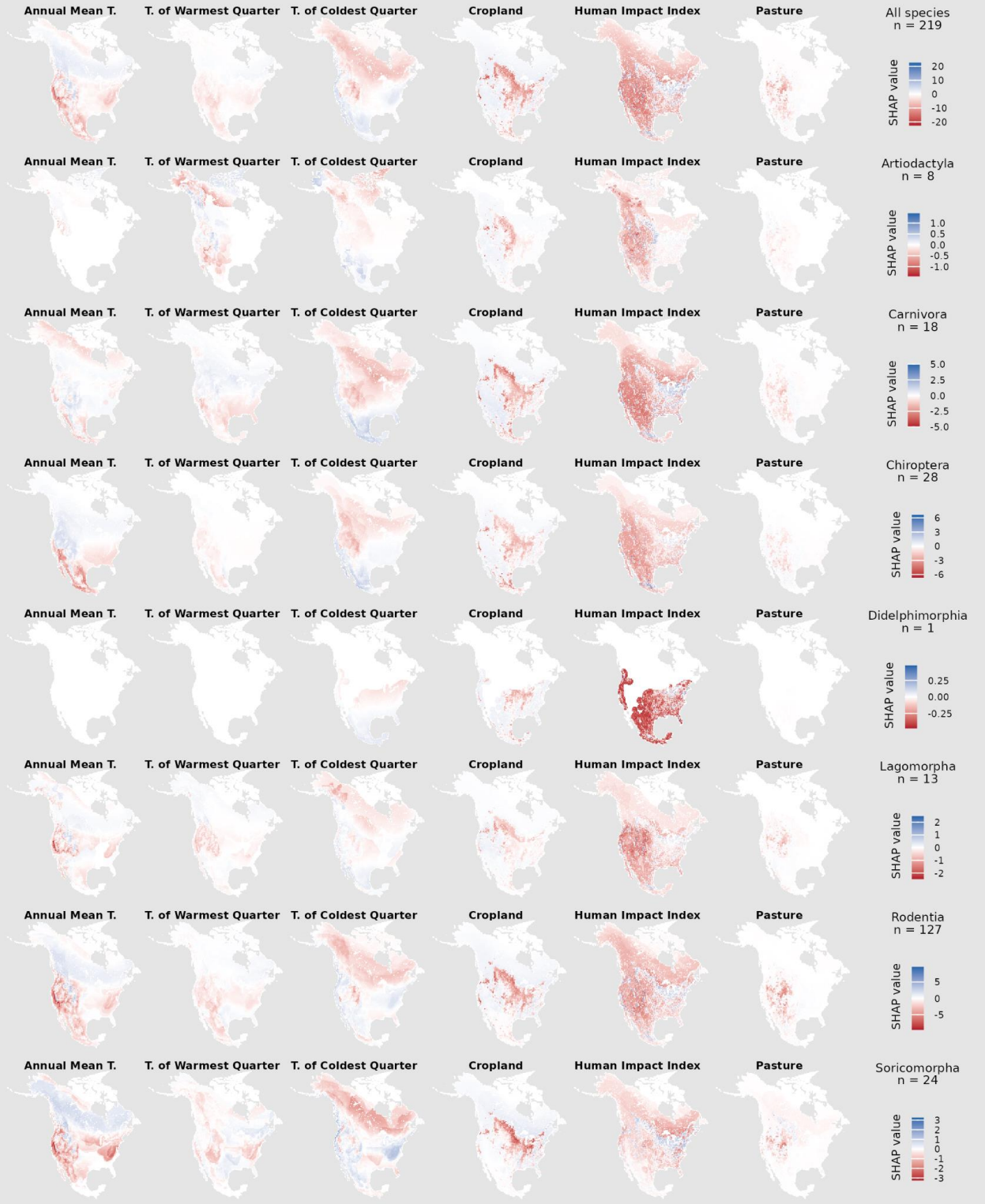

Figure 4. Aggregated SHAP maps for the three top-contributing climatic factors and the three top-contributing anthropogenic factors. SHAP values are aggregated across all species (n = 219) and separately within each mammal order. Blue indicates positive SHAP values, red indicates negative SHAP values, and white indicates zero. Aggregated SHAP maps for all factors are shown in Figure S19.

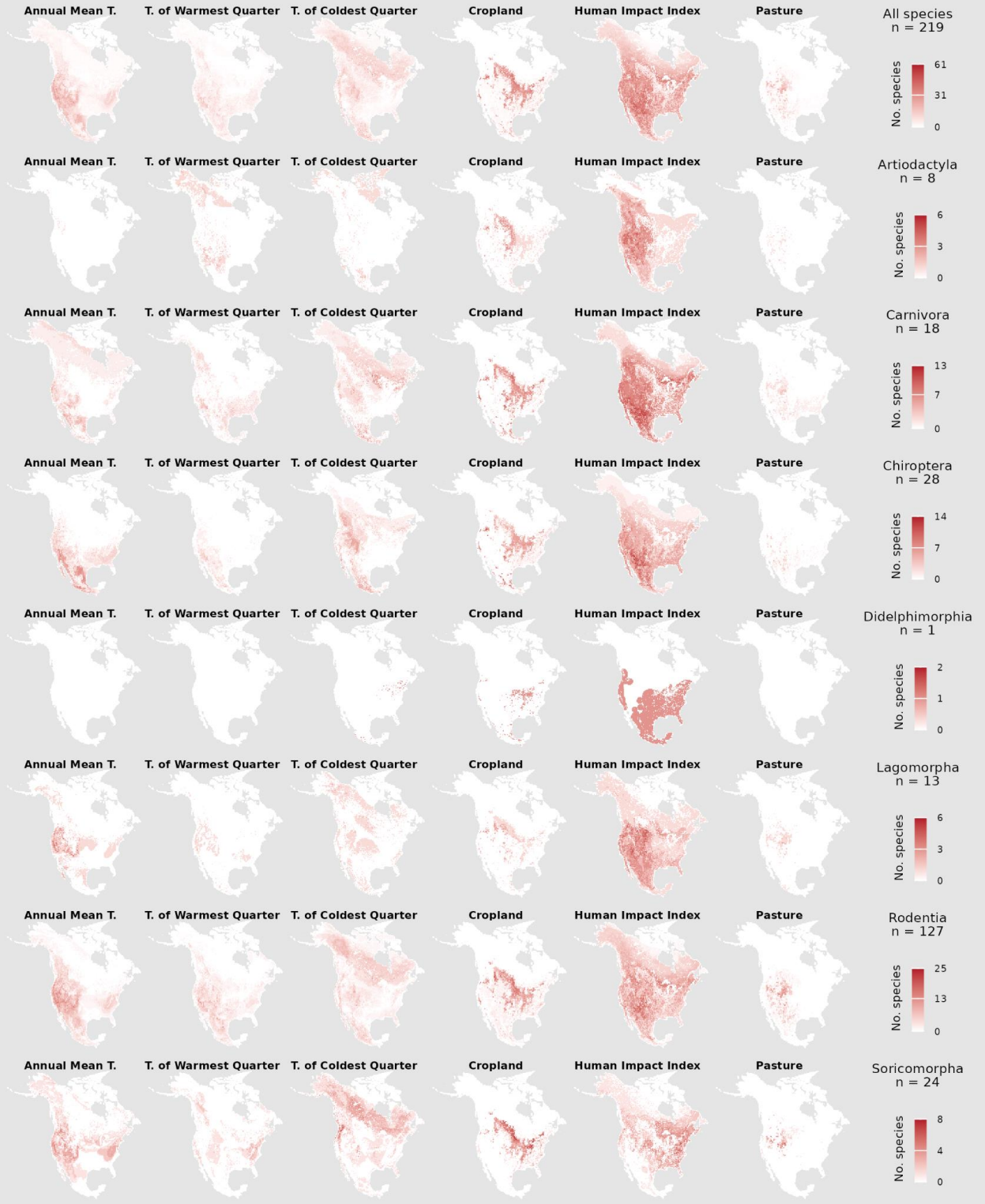

Figure 5. Frequency maps of locally dominating effects for six environmental factors. For each species and raster cell, the factor with the largest absolute SHAP value is identified as the locally dominant factor. Maps show the number of species for which each factor is locally dominant, summarized across all species (n = 219) and separately within each mammal order. Darker red indicates a larger number of species for which that factor is the dominant factor.

Results are shown for the three top-contributing climatic factors and the three top-contributing anthropogenic factors; maps for all dominant factors are provided in Figure S20.

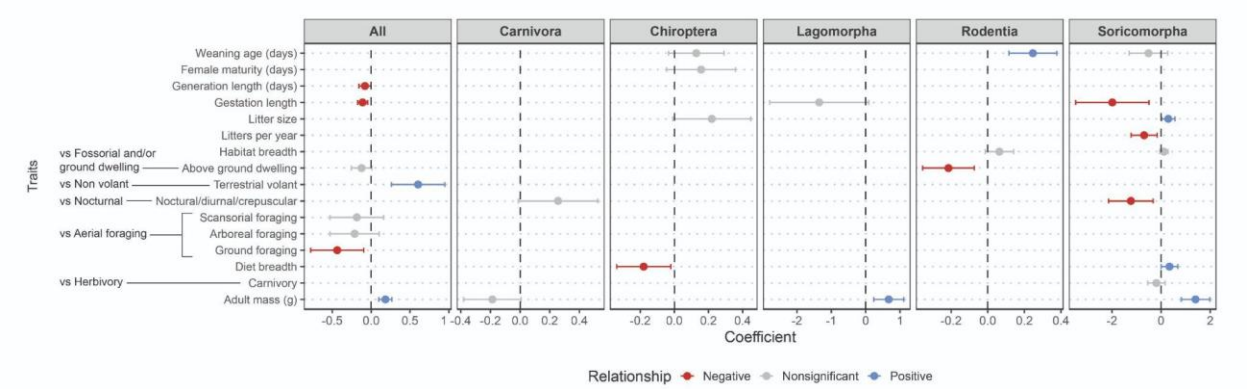

Figure 6. Relationships between the responses to human impact index (HII) and mammal traits. The panels show the estimated coefficients of the linear regression for the stepwise-selected models based on AIC. The response variable is each species' cumulative responses to HII and the predictor variables are the biological traits of modeled species (see Methods). The models are performed for all species and different mammal orders. The control group of a factorial trait is labeled along the y-axis. The predictors are labeled as blue (the estimated coefficient is positive and is significantly different from zero), red (the estimated coefficient is negative and is significantly different from zero), and gray (the estimated coefficient is not significantly different from zero).

References:

AdaptWest Project. (2022). Gridded current and projected climate data for North America at 1km resolution, generated using the *ClimateNA v7.30* software (T. Wang et al., 2022).

de Andrade, A.C. (2022). Density of marmosets in highly urbanised areas and the positive effect of arboreous vegetation. *Urban Ecosyst.*, 25, 101–109.

Andrewartha, H.G. & Birch, C. (1954). *The Distribution and Abundance of Animals. University of Chicago Press*.

Aulus-Giacosa, L., Ollier, S. & Bertelsmeier, C. (2024). Non-native ants are breaking down biogeographic boundaries and homogenizing community assemblages. *Nat. Commun.*, 15, 2266.

Barredo Arrieta, A., Díaz-Rodríguez, N., Del Ser, J., Bennetot, A., Tabik, S., Barbado, A., *et al.* (2020). Explainable Artificial Intelligence (XAI): Concepts, taxonomies, opportunities and challenges toward responsible AI. *Inf. Fusion*, 58, 82–115.

Bateman, P.W. & Fleming, P.A. (2012). Big city life: carnivores in urban environments. *J. Zool.* , 287, 1–23.

Bennett, V.J. (2017). Effects of Road Density and Pattern on the Conservation of Species and Biodiversity. *Current Landscape Ecology Reports*, 2, 1–11.

Berman, L.M., Schneider, F.D., Pavlick, R.P., Stenglein, J., Bemowski, R., Dean, M., & Townsend, P.A. (2024). Fractional Richness: An index for camera trap networks. *Ecol. Indic.*, 166, 112266.

Bielby, J., Mace, G.M., Bininda-Emonds, O.R.P., Cardillo, M., Gittleman, J.L., Jones, K.E., *et al.* (2007). The fast-slow continuum in mammalian life history: an empirical reevaluation. *Am. Nat.*, 169, 748–757.

Boria, R.A., Olson, L.E., Goodman, S.M. & Anderson, R.P. (2014). Spatial filtering to reduce sampling bias can improve the performance of ecological niche models. *Ecol. Modell.*, 275, 73–77.

Burton, A.C., Beirne, C., Gaynor, K.M., Sun, C., Granados, A., Allen, M.L., *et al.* (2024). Mammal responses to global changes in human activity vary by trophic group and landscape. *Nat Ecol Evol*, 8, 924–935.

Capinha, C., Essl, F., Seebens, H., Moser, D. & Pereira, H.M. (2015). BIOGEOGRAPHY. The dispersal of alien species redefines biogeography in the Anthropocene. *Science*, 348, 1248–1251.

Caro, T., Rowe, Z., Berger, J., Wholey, P. & Dobson, A. (2022). An inconvenient misconception: Climate change is not the principal driver of biodiversity loss. *Conserv. Lett.*, 15, e12868.

Chapman, S., Mustin, K., Renwick, A.R., Segan, D.B., Hole, D.G., Pearson, R.G., *et al.* (2014). Publishing trends on climate change vulnerability in the conservation literature reveal a predominant focus on direct impacts and long time-scales. *Divers. Distrib.*, 20, 1221–1228.

Cheeseman, A.E., Jachowski, D.S. & Kays, R. (2024). From past habitats to present threats: tracing North American weasel distributions through a century of climate and land use change. *Landsc. Ecol.*, 39, 104.

Chen, X., Liang, Y., & Feng, X. (2024). Influence of model complexity, training collinearity, collinearity shift, predictor novelty and their interactions on ecological forecasting. *Glob. Ecol. Biogeogr.*, 33, 371–384.

Corrêa, F.M., Chaves, Ó.M., Printes, R.C. & Romanowski, H.P. (2018). Surviving in the

urban-rural interface: Feeding and ranging behavior of brown howlers (Alouatta guariba clamitans) in an urban fragment in southern Brazil. *Am. J. Primatol.*, 80, e22865.
Cristaldi, M.A., Giraudo, A.R., Arzamendia, V., Bellini, G.P. & Claus, J. (2017). Urbanization impacts on the trophic guild composition of bird communities. *J. Nat. Hist.*, 51, 2385–2404.
Dormann, C.F., Elith, J., Bacher, S., Buchmann, C., Carl, G., Carré, G., *et al.* (2013). Collinearity: a review of methods to deal with it and a simulation study evaluating their performance. *Ecography* , 36, 27–46.
Elith, J., H. Graham, C., P. Anderson, R., Dudík, M., Ferrier, S., Guisan, A., *et al.* (2006). Novel methods improve prediction of species' distributions from occurrence data. *Ecography*, 29, 129–151.
Faurby, S., Davis, M., Pedersen, R.Ø., Schowanek, S.D., Antonelli, A., & Svenning, J.-C. (2018). PHYLACINE 1.2: The Phylogenetic Atlas of Mammal Macroecology. *Ecology*, 99, 2626.
Faurby, S., Pedersen, R. Ø., Davis, M., Schowanek, S. D., Jarvie, S., Antonelli, A., & Svenning, J.-C. (2020). MegaPast2Future/PHYLACINE_1.2: PHYLACINE Version 1.2.1. Zenodo. https://doi.org/10.5281/ZENODO.3690867
Fedriani, J.M., Fuller, T.K. & Sauvajot, R.M. (2001). Does availability of anthropogenic food enhance densities of omnivorous mammals? An example with coyotes in southern California. *Ecography* , 24, 325–331.
Feng, X., Enquist, B.J., Park, D.S., Boyle, B., Breshears, D.D., Gallagher, R.V., *et al.* (2022). A review of the heterogeneous landscape of biodiversity databases: Opportunities and challenges for a synthesized biodiversity knowledge base. *Glob. Ecol. Biogeogr.*, 31, 1242–1260.
Feng, X., Park, D.S., Liang, Y., Pandey, R. & Papeş, M. (2019a). Collinearity in ecological niche modeling: Confusions and challenges. *Ecol. Evol.*, 9, 10365–10376.
Feng, X., Park, D.S., Walker, C., Peterson, A.T., Merow, C. & Papeş, M. (2019b). A checklist for maximizing reproducibility of ecological niche models. *Nat Ecol Evol*, 3, 1382–1395.
Feng, X., Peterson, A.T., Aguirre-López, L.J., Burger, J.R., Chen, X. & Papeş, M. (2024). Rethinking ecological niches and geographic distributions in face of pervasive human influence in the Anthropocene. *Biol. Rev.*, 99, 1481–1503.
Finn, C., Grattarola, F. & Pincheira-Donoso, D. (2023). More losers than winners: investigating Anthropocene defaunation through the diversity of population trends. *Biol. Rev.*, 98, 1732–1748.
Fitzpatrick, M.C., Gotelli, N.J. & Ellison, A.M. (2013). MaxEnt versus MaxLike: empirical comparisons with ant species distributions. *Ecosphere*, 4, 1–15.
Forman, R.T.T., Sperling, D., Bissonette, J.A., Clevenger, A.P., Cutshall, C.D., Dale, V.H., *et al.* (2003). *Road ecology: Science and solutions*. Island press Washington, DC.
Franklin, J., Regan, H.M. & Syphard, A.D. (2014). Linking spatially explicit species distribution and population models to plan for the persistence of plant species under global change. *Environ. Conserv.*, 41, 97–109.
Frans, V.F. & Liu, J. (2024). Gaps and opportunities in modelling human influence on species distributions in the Anthropocene. *Nat. Ecol. Evol.*, 8, 1365–1377.
Gallardo, B. & Aldridge, D.C. (2013). The "dirty dozen": socio-economic factors amplify the invasion potential of 12 high-risk aquatic invasive species in Great Britain and Ireland.

J. Appl. Ecol., 50, 757–766.
Gallardo, B., Zieritz, A. & Aldridge, D.C. (2015). The importance of the human footprint in shaping the global distribution of terrestrial, freshwater and marine invaders. *PLoS One*, 10, e0125801.
Gallego-Zamorano, J., Benítez-López, A., Santini, L., Hilbers, J.P., Huijbregts, M.A.J. & Schipper, A.M. (2020). Combined effects of land use and hunting on distributions of tropical mammals. *Conserv. Biol.*, 34, 1271–1280.
Gao, J. & O'Neill, B.C. (2020). Mapping global urban land for the 21st century with data-driven simulations and Shared Socioeconomic Pathways. *Nat. Commun.*, 11, 2302.
Gaynor, K.M., Hojnowski, C.E., Carter, N.H. & Brashares, J.S. (2018). The influence of human disturbance on wildlife nocturnality. *Science*, 360, 1232–1235.
GBIF.org. (2023). GBIF Occurrence Download. *GBIF Occurrence Download*.
Grilo, C., Koroleva, E., Andrášik, R., Bíl, M. & González-Suárez, M. (2020). Roadkill risk and population vulnerability in European birds and mammals. *Front. Ecol. Environ.*, 18, 323–328.
Guarnieri, M., Kumaishi, G., Brock, C., Chatterjee, M., Fabiano, E., Katrak-Adefowora, R., *et al.* (2024). Effects of climate, land use, and human population change on human–elephant conflict risk in Africa and Asia. *Proc. Natl. Acad. Sci. U.S.A.*, 121, e2312569121.
Guiry, E. & Buckley, M. (2018). Urban rats have less variable, higher protein diets. *Proc. Biol. Sci.*, 285, 20181441.
Helmus, M.R., Mahler, D.L. & Losos, J.B. (2014). Island biogeography of the Anthropocene. *Nature*, 513, 543–546.
Hommel, G. (1988). A stagewise rejective multiple test procedure based on a modified bonferroni test. *Biometrika*, 75, 383.
Howard, C., Flather, C.H. & Stephens, P.A. (2020). A global assessment of the drivers of threatened terrestrial species richness. *Nat. Commun.*, 11, 993.
Hughes, A.C., Orr, M.C., Ma, K., Costello, M.J., Waller, J., Provoost, P., *et al.* (2021). Sampling biases shape our view of the natural world. *Ecography* , 44, 1259–1269.
Jiang, D., Zhao, X., López-Pujol, J., Wang, Z., Qu, Y., Zhang, Y., Zhang, T., Li, D., Jiang, K., Wang, B., Yan, C., & Li, J.-T. (2023). Effects of climate change and anthropogenic activity on ranges of vertebrate species endemic to the Qinghai-Tibet Plateau over 40 years. *Conserv. Biol.*, 37, e14069.
Kays, R., Snider, M.H., Hess, G., Cove, M.V., Jensen, A., Shamon, H., *et al.* (2024). Climate, food and humans predict communities of mammals in the United States. *Divers. Distrib.*, 30, e13900.
Kunz, T.H. (1974). Reproduction, growth, and mortality of the vespertilionid bat, Eptesicus fuscus, in Kansas. *J. Mammal.*, 55, 1–13.
Lamb, C.T., Mowat, G., McLellan, B.N., Nielsen, S.E. & Boutin, S. (2017). Forbidden fruit: human settlement and abundant fruit create an ecological trap for an apex omnivore. *J. Anim. Ecol.*, 86, 55–65.
Larson, R.N., Brown, J.L., Karels, T. & Riley, S.P.D. (2020). Effects of urbanization on resource use and individual specialization in coyotes (Canis latrans) in southern California. *PLoS One*, 15, e0228881.
Lewis, S. L., & Maslin, M. A. (2015). Defining the anthropocene. Nature, 519, 171–180.
Li, C., Fang, Y.-H., Ren, G.-P., Li, Y.-P., Huang, Z.-P., Cui, L.-W., Youlatos, D., Garber, P. A., Ni, X.-J., Zhu, H., Luo, D.-W., Liu, X., Chu-Yuan, M.-R., Tian, Y.-P., Li, Y.-C., Zeng,

X.-L., Yan, D., Li, G.-H., Xiao, W., … Yang, Y. (2025). Monsoon climate and anthropogenic influences shape primate distributions across the southeastern edge of the Qinghai-Tibet Plateau. *Glob. Chang. Biol.*, 31, e70178.
Li, X., Hu, W., Bleisch, W.V., Li, Q., Wang, H., Lu, W., *et al.* (2022). Functional diversity loss and change in nocturnal behavior of mammals under anthropogenic disturbance. *Conserv. Biol.*, 36, e13839.
Li, X., Zhou, Y., Hejazi, M., Wise, M., Vernon, C., Iyer, G., *et al.* (2021). Global urban growth between 1870 and 2100 from integrated high resolution mapped data and urban dynamic modeling. *Commun. Earth Environ.*, 2, 1–10.
Lomolino, M.V., Riddle, B.R., Whittaker, R.J. & Brown, J.H. (2010). *Biogeography. 4th edition. Sinauer Associates*. 4th edn. Sinauer Associates.
Lundberg, S. & Lee, S.-I. (2017). A unified approach to interpreting model predictions. *arXiv [cs.AI]*.
MacArthur, R.H. (1984). *Geographical Ecology: Patterns in the Distribution of Species. Princeton University Press*. Princeton University Press.
Merow, C., Smith, M.J. & Silander, J.A., Jr. (2013). A practical guide to MaxEnt for modeling species' distributions: what it does, and why inputs and settings matter. *Ecography* , 36, 1058–1069.
Montràs-Janer, T., Suggitt, A. J., Fox, R., Jönsson, M., Martay, B., Roy, D. B., Walker, K. J., & Auffret, A. G. (2024). Anthropogenic climate and land-use change drive short- and long-term biodiversity shifts across taxa. *Nat. Ecol. Evol.*, 8, 739–751.
Neves, M.P., Delariva, R.L., Perkins, D.M., Fialho, C.B. & Kratina, P. (2024). Trophic plasticity of omnivorous fishes in natural and human-dominated landscapes. *Limnol. Oceanogr.*, 69, 189–202.
Oro, D., Genovart, M., Tavecchia, G., Fowler, M.S. & Martínez-Abraín, A. (2013). Ecological and evolutionary implications of food subsidies from humans. *Ecol. Lett.*, 16, 1501–1514.
Pacifici, M., Rondinini, C., Rhodes, J.R., Burbidge, A.A., Cristiano, A., Watson, J.E.M., *et al.* (2020). Global correlates of range contractions and expansions in terrestrial mammals. *Nat. Commun.*, 11, 2840.
Parkins, K.L. & Clark, J.A. (2015). Green roofs provide habitat for urban bats. *Glob. Ecol. Conserv.*, 4, 349–357.
Pergams, O.R.W. & Lawler, J.J. (2009). Recent and widespread rapid morphological change in rodents. *PLoS One*, 4, e6452.
Peterson, A. T., Papeş, M., & Soberón, J. (2015). Mechanistic and correlative models of ecological niches. *Eur. J. Ecol.*, 1, 28–38.
Phillips, S.J. (2005). A brief tutorial on Maxent. *At&t Research*, 190, 231–259.
Phillips, S.J. & Dudík, M. (2008). Modeling of species distributions with Maxent: new extensions and a comprehensive evaluation. *Ecography* , 31, 161–175.
Phillips, S.J., Dudík, M., Elith, J., Graham, C.H., Lehmann, A., Leathwick, J., *et al.* (2009). Sample selection bias and presence-only distribution models: implications for background and pseudo-absence data. *Ecol. Appl.*, 19, 181–197.
Pineda-Munoz, S., Wang, Y., Lyons, S.K., Tóth, A.B. & McGuire, J.L. (2021). Mammal species occupy different climates following the expansion of human impacts. *Proc. Natl. Acad. Sci. U. S. A.*, 118.
Relyea, R. & Ricklefs, R.E. (2013). *The Economy of Nature: Seventh Edition*. Macmillan

Learning.
Revell, L. J. (2010). Phylogenetic signal and linear regression on species data: Phylogenetic regression. *Methods Ecol. Evol.*, 1, 319–329.
Revell, L. J. (2024). phytools 2.0: an updated R ecosystem for phylogenetic comparative methods (and other things). *PeerJ*, 12, e16505.
Richardson, J.L., Michaelides, S., Combs, M., Djan, M., Bisch, L., Barrett, K., *et al.* (2021). Dispersal ability predicts spatial genetic structure in native mammals persisting across an urbanization gradient. *Evol. Appl.*, 14, 163–177.
Sakai, A.K., Allendorf, F.W., Holt, J.S., Lodge, D.M., Molofsky, J., With, K.A., *et al.* (2001). The Population Biology of Invasive Species. *Annu. Rev. Ecol. Evol. Syst.*, 32, 305–332.
Sandom, C., Faurby, S., Sandel, B. & Svenning, J.-C. (2014). Global late Quaternary megafauna extinctions linked to humans, not climate change. *Proc. Biol. Sci.*, 281.
Santini, L., Pironon, S., Maiorano, L. & Thuiller, W. (2019). Addressing common pitfalls does not provide more support to geographical and ecological abundant-centre hypotheses. *Ecography* , 42, 696–705.
Shapley, L.S. (1953). 17. A Value for n-Person Games. In: *Contributions to the Theory of Games (AM-28), Volume II* (eds. Kuhn, H.W. & Tucker, A.W.). Princeton University Press, Princeton, pp. 307–318.
Smith, A.B., Murphy, S.J., Henderson, D. & Kelley D. Erickson, K.D. (2023). Including Imprecisely Georeferenced Specimens Improves Accuracy of Species Distribution Models and Estimates of Niche Breadth. *Glob. Ecol. Biogeogr.*, 32, 342–355.
Smith, A.B. & Maria J. Santos. 2020. Testing the Ability of Species Distribution Models to Infer Variable Importance. *Ecography*, 43, 1801–1813.
Smith, F.A. & Lyons, S.K. (2011). How big should a mammal be? A macroecological look at mammalian body size over space and time. *Proc. Biol. Sci.*, 366, 2364–2378.
Soga, M. & Gaston, K.J. (2020). The ecology of human-nature interactions. *Proc. Biol. Sci.*, 287, 20191882.
Song, L. & Estes, L. (2023). itsdm : Isolation forest-based presence-only species distribution modelling and explanation in r. *Methods Ecol. Evol.*, 14, 831–840.
Soria, C.D., Pacifici, M., Di Marco, M., Stephen, S.M. & Rondinini, C. (2021). COMBINE: a coalesced mammal database of intrinsic and extrinsic traits. *Ecology*, 102, e03344.
Steffen, W., Broadgate, W., Deutsch, L., Gaffney, O. & Ludwig, C. (2015). The trajectory of the Anthropocene: The Great Acceleration. *Anthropocene Rev.*, 2, 81–98.
Strobl, C., Boulesteix, A.-L., Zeileis, A. & Hothorn, T. (2007). Bias in random forest variable importance measures: illustrations, sources and a solution. *BMC Bioinformatics*, 8, 25.
Suraci, J.P., Gaynor, K.M., Allen, M.L., Alexander, P., Brashares, J.S., Cendejas-Zarelli, S., *et al.* (2021). Disturbance type and species life history predict mammal responses to humans. *Glob. Chang. Biol.*, 27, 3718–3731.
Treves, A. & Karanth, K.U. (2003). Human-carnivore conflict and perspectives on carnivore management worldwide. *Conserv. Biol.*, 17, 1491–1499.
Tryjanowski, P., Morelli, F., & Møller, A. P. (2020). Urban birds. In *The Routledge Handbook of Urban Ecology* (pp. 399–411). Routledge.
https://doi.org/10.4324/9780429506758-34
Tucker, M.A., Santini, L., Carbone, C. & Mueller, T. (2021). Mammal population densities

at a global scale are higher in human-modified areas. *Ecography* , 44, 1–13.
Van Scoyoc, A., Smith, J.A., Gaynor, K.M., Barker, K. & Brashares, J.S. (2023). The influence of human activity on predator-prey spatiotemporal overlap. *J. Anim. Ecol.*, 92, 1124–1134.
Venter, O., Sanderson, E.W., Magrach, A., Allan, J.R., Beher, J., Jones, K.R., *et al.* (2016). Sixteen years of change in the global terrestrial human footprint and implications for biodiversity conservation. *Nat. Commun.*, 7, 12558.
Waldock, C., Wegscheider, B., Josi, D., Calegari, B.B., Brodersen, J., Jardim de Queiroz, L., *et al.* (2024). Deconstructing the geography of human impacts on species' natural distribution. *Nat. Commun.*, 15, 8852.
Williams, J. J., & Newbold, T. (2021). Vertebrate responses to human land use are influenced by their proximity to climatic tolerance limits. *Divers. Distrib.*, 27, 1308–1323.
Yalden, D.W. & Morris, P.A. (1975). *The Lives of Bats*. David & Charles.
Yue, X., Hughes, A.C., Tomlinson, K.W., Xia, S., Li, S. & Chen, J. (2019). Body size and diet–related morphological variation of bats over the past 65 years in China. *J. Mammal.*, 101, 61–79.

Supplementary Materials

Supplementary Methods

Figures S1-17

Tables S1-S5

Supplementary Methods

Occurrence data

Our study focused on mammal species whose geographic ranges are mainly (> 70%) in North America, where large amounts of species observational records have been collected (Feng *et al.* 2022; Hughes *et al.* 2021). We used this criterion to identify species that have abundant observation data across their ranges, thus to make more robust inferences on the relationship between species distribution and climatic or anthropogenic factors. We downloaded expert range maps of all mammal species from the International Union for Conservation of Nature ("IUCN" 2022), and used IUCN polygons coded as native and reintroduced (i.e., historical ranges) to intersect with the main continent of North America. This step led to 509 mammal species whose geographic ranges are mainly in North America. We downloaded the presence records of these species from the Global Biodiversity Information Facility (GBIF) database (GBIF.org 2023). We filtered the presence records based on the basis of records and only kept records coded as preserved specimen, human observation, occurrence, material citation, machine observation, and material sample (see the treatment and sensitivity analysis of sampling bias below). We retained the presence records that were collected between 1990 and 2020 to represent the more recent distribution of the focal species; this temporal extent was also aligned with that of the environmental variables to be used in the ecological niche model (Feng *et al.* 2019b). We excluded the presences that were outside of slightly enlarged IUCN range maps (buffered by 1/10 of the radius of a range map assuming its circular shape) to avoid potential vagrant records. The buffered IUCN range was subsequently used as the modeling domain for each species. We applied spatial thinning to the occurrence data and only kept one occurrence in each 10 km grid to minimize the impact of sampling bias (Boria *et al.* 2014). We further excluded species with less than 50 spatially unique presence records to ensure more robust model performance (Papeş & Gaubert 2007). We also excluded species that have relatively low model evaluation metrics. Following the criteria discussed above, we retained a list of 219 species (Table S1, Fig. S1) for investigating the influence of climatic and anthropogenic factors on their distributions.

Bioclimatic and anthropogenic factors

For the ecological models, we selected six out of 19 bioclimatic variables that are commonly used in ecological niche modeling literature, and selected 6 out of 25 representative anthropogenic factors that may potentially affect species' geographic distributions compiled in (Feng *et al.* 2024). The six bioclimatic factors were annual mean temperature (Annual mean T), annual precipitation (Annual P), mean temperature of warmest/coldest quarter (Maximum/Minimum T), and precipitation of wettest/driest quarter (Wettest/Driest P) (Table S2). These variables represent the mean and extreme climatic conditions that are widely recognized for their effects in determining species' geographic distributions (Lomolino *et al.* 2010). We calculated these bioclimatic variables based on monthly climatic data between 1990-2020 at 1 km spatial resolution downloaded from AdaptWest database (AdaptWest Project 2022) using 'dismo' package Version 1.3-5 (Hijmans *et al.* 2017) in R (v4.3.2) (R Core Team 2024).

The six representative anthropogenic factors were human impact index (HII), highway density, cropland percentage (Cropland), pasture percentage (Pasture), nighttime lights, and human population (Table S2). We selected six variables based on the type of human stressors they represent, while avoiding high correlation [correlation coefficient $|r| < 0.7$, Fig. S2; (Dormann *et*

al. 2013; Feng *et al.* 2019a)] among them and better matching their temporal extents (2010-2018) to those of species' occurrence and climatic data. These variables have been found to influence mammalian distributions from regional to global scales (Burton *et al.* 2024; Cheeseman *et al.* 2024; Guarnieri *et al.* 2024; Tucker *et al.* 2021). The human impact index is a type of synthetic variable that builds upon multiple human stressors that include population density, land cover/land use, built infrastructure (such as roads, railways, housing, parking lots, power lines, and barns), human accessibility (derived from distance to roads, waterways, and coasts), and power consumption (derived from nighttime light) (Sanderson *et al.* 2022). HII is similar to human footprint, another synthetic index of human impacts, which is known to be influential to species geographic distributions (Gallardo *et al.* 2015; Pacifici *et al.* 2020; Suraci *et al.* 2021). The development of HII built upon the consistent methodology with "first-generation" human footprint, but was further enhanced with higher spatial resolution, more frequently updated, and better thematically resolved datasets (Sanderson *et al.* 2022). This integrated measure of human impacts has been found important for explaining large-scale native (Kays *et al.* 2024; Suraci *et al.* 2021) and invasive terrestrial animals (Gallardo *et al.* 2015). Highways and other major roads can prevent animal dispersal (Forman *et al.* 2003) and have a detrimental impact on animal abundance (Fahrig & Rytwinski 2009). Croplands and pastures are known to be associated with mammal species' distribution loss (Gallego-Zamorano *et al.* 2020), but also have positive impacts by providing additional food resources to harbor generalist small-mammal species (Shilereyo *et al.* 2023). Artificial nighttime lights reflect the intensities of high human activities (Tucker *et al.* 2021) and can widely influence the mammal activity patterns (Gaynor *et al.* 2018). Lastly, human population density was used to represent human pressures (Pyšek *et al.* 2010) and disturbances in human-modified areas because of its important association with mammal densities (Tucker *et al.* 2021). The selected variables encompassed a wide spectrum of human impacts, allowing a more comprehensive comparison of human impacts against those of climate in shaping present mammalian distributions across North America. All environmental layers were aligned with North America at 1 km spatial resolution.

Modeling

We performed ecological niche models using the Maxent algorithm (version 3.4.3). Maxent estimates the relationship between species' distribution and environmental conditions by computing the maximum likelihood of species' presence using the Gibbs probability distribution with the maximum entropy, constrained to empirical averages of environmental variables (Phillips *et al.* 2004). Maxent effectively handles presence-background data and has demonstrated consistently high accuracy in modeling a variety of species distributions (Elith *et al.* 2006; Phillips & Dudík 2008). We included linear and quadratic features to avoid overly complex response functions to ensure ecologically relevant interpretation of the relationship between species' geographic distribution and environmental predictors (Merow *et al.* 2013). The default regularization parameters of Maxent were used. To account for sampling bias that may occur in the occurrence data (e.g., research-grade data from iNaturalist that are part of the GBIF download), we generated target group background data with the same underlying bias as the occurrence data for each species (Phillips *et al.* 2009). The selection of 10,000 target group background points was weighted by the sampling bias surface of occurrences obtained through kernel density estimation (Fitzpatrick *et al.* 2013). The sampling bias surface was restricted within the modeling domain (i.e., buffered IUCN range) for each species. For 21 species with restricted ranges (i.e., modeling domain < 10,000 pixels), all pixels were used. Besides using

target group background data, we performed an additional sensitivity analysis to evaluate the impact of potential sampling bias in the model outcomes; we repeated the modeling experiment by excluding all human observations (mostly data from iNaturalist) and obtained largely consistent results (Figs. S3 & S10).

To assess model performance, we performed 5-fold cross-validation by partitioning occurrence data of each species into training (80%) and test (20%) datasets. Maxent was fitted using the training occurrences and previously selected target group background points, and was evaluated using testing occurrences and 10,000 background points (or all pixels when the modeling domain had < 10,000 pixels) randomly drawn from the modeling domain. Note that random background points were used in the evaluation, which makes the interpretation of the x-axis of the AUC curve to be the proportion of areas predicted to be present (as opposed to the false positive rate when true absences are used) (Peterson *et al.* 2008); a similar methodology has been used by (Fitzpatrick *et al.* 2013). We evaluated model performance using the area under the receiver operating characteristic curve (AUC) and continuous Boyce index (CBI). AUC is a threshold-independent evaluation index ranging from 0 to 1, with values above 0.5 indicating models better than random (Swets 1979). CBI measures model accuracy and is appropriate for evaluating models with presence-background data (Hirzel *et al.* 2006). Both AUC and CBI were averaged over 5-fold cross validation. To ensure the robustness of the results, we excluded species with relatively low model performance (mean AUC ≤ 0.6 or mean CBI ≤ 0), and proceeded with the full models of 219 species in the subsequent analyses.

We used permutation importance of each variable to represent its contribution to the ecological niche model. The permutation importance of a variable is the amount of decrease in training AUC when the values of a focal variable were permuted. Larger values of permutation importance indicate greater variable importance in modeling the relationship between species' distribution and environmental conditions. The permutation importance is typically normalized to percentages, running from 0 to 100% (Phillips 2005). Here we used permutation importance to compare the relative contribution of anthropogenic factors versus bioclimatic factors. The influence of collinearity on the permutation importance was expected to be minimal, as the predictors included were not highly correlated (Strobl *et al.* 2007) (Fig. S2). In addition, we also calculated the rank of variable contribution, ranging from 1, meaning most important, to 12, meaning least important.

We performed two additional experiments to evaluate the robustness of the modeling results toward the choice of modeling algorithm and variable collinearity. First, we fit boosted regression trees (BRT) (Elith *et al.* 2008), another machine learning algorithm, using the same 12 predictor variables as used in Maxent for each species. Second, we investigated whether the collinearity among bioclimatic variables (Fig. S2) had an influence on the comparison of permutation variable importance between anthropogenic and bioclimatic factors. To do so, we applied principal component analysis to all 19 bioclimatic variables and obtained permutation variable importance by calibrating Maxent with six selected anthropogenic factors and six bioclimatic principal components (PCs) for each species. Note that the selection of the six anthropogenic factors avoided high correlation; thus, no principal component analysis was used on anthropogenic factors. We found similar patterns of variable importance from the two experiments.

Response to human impacts in environmental and geographic space

In our preliminary analysis, HII stood out to be highly important for most mammal species. Therefore, we further investigated the response curve of HII for each species. The response curve represents the predicted relative probability of presence of a species given a gradient of an environmental variable, which is HII in this case. To compare the response curve of all species, the response curve was projected to the range of HII values available in North America using the'enmSdmX' package (Smith 2022). We note that model extrapolation was involved when constructing the response curves, though we considered the risk to be relatively low. The breadth of HII values used in model training is relatively wide. The mean minimum and maximum HII values of all species investigated were 0.05 (sd=0.51) and 5024.79 (sd=438.70), respectively, which are very close to the range of HII in the study area (0-5865; Fig. S13). Also, we only included linear and quadratic features during model training to avoid overly complex response functions; thus, we expect the selected strategy to be less prone to extrapolation risk compared with more complex response curves (Chen et al. 2024).

We categorized the response curves into five groups (I, II, III, IV, V), reflecting the different levels of HII where the relative probability of presence for a species reaches the highest value. More specifically, we derived one response index for each curve. The response index considered the proportion of segments with positive slopes and the position where the predicted relative probability of presence peaked. Each response curve was evenly separated into 5865 segments (5865 is the maximum value of HII in the study area). The index will reach a maximum value of 3 when a monotonically increasing response curve peaks at the top-right corner (i.e., relative probability of presence = 1 and HII = 5865). Based on the response indices, we performed a cluster analysis using k-means based on the 'stats' package in R. The number of groups (i.e., five) was determined using the 'factoextra' package, which explored different numbers of groups (k); there was a sharp decline of within-cluster sums of squares from k = 1 to k = 4, followed by a smaller reduction after k = 5, indicating that five clusters provide a reasonable explanation for variation in response-curve structure and avoid over-partitioning (Fig. S14). Such grouping (I, II, III, IV, V) is analogous to the concepts of urban avoider, urban adapter, and urban exploiter, or human-sensitive species, intermediate species, and human-associated species (Berman et al., 2024).

We also generated SHapley Additive exPlanations (SHAP) (Lundberg & Lee 2017; Shapley 1953) maps to show species' response to environmental factors across the geographic space. SHAP is one of the explainable artificial intelligence (xAI) tools that provides an interpretation of the covariate effect on the predicted outcome at the observation level (here, a grid cell). A SHAP value indicates the difference between what a variable contributes to a prediction in each location, and what the variable is expected to contribute given the mean model prediction. Compared with permutation importance, a SHAP value represents a predictor's contribution to the prediction for that specific grid cell, i.e., the location-specific effect of each predictor (Waldock *et al.* 2024). A SHAP value of 0 suggests no contribution, while a deviation from 0 indicates a larger positive or negative contribution. We calculated SHAP values for each of the 12 variables used in the main modeling experiment across the modeling domain of a focal species using the R package 'itsdm' with 100 times of simulations (Song & Estes 2023). For every species, there would be 12 layers of SHAP maps, each representing a variable. We

aggregated the SHAP maps for each variable and each mammal order to illustrate the overall importance of a focal variable. The aggregation was performed at 40-km spatial resolution to facilitate the visual comparison across groups. We also identified cases where a focal variable has the highest absolute SHAP value at a focal pixel (among SHAP values of all 12 variables at the same pixel); this was performed for each pixel across each species' geographic range, and aggregated across different mammal orders or all species.

Traits data

To further investigate whether species' response to HII was affected by their biological traits, we compiled a set of mammal traits from the COMBINE database (Soria *et al.* 2021). Overall, we selected the trait data that are known to be strong predictors of mammals' response to human impacts and that are available for the 331 species (Table S3). We avoided trait variables that were highly correlated. The 15 selected traits include: 1) body mass, 2) female sexual maturity, 3) gestation length, 4) litter size, 5) number of litters, 6) weaning age, 7) generation length, 8) hibernation or torpor, 9) diet breadth, 10) habitat breadth, 11) trophic level, 12) foraging strata, 13) fossoriality, 14) activity cycle, and 15) volant capacity. Body mass is a notable factor broadly used in macroecology and biogeography that determines species response to various environmental factors; larger-bodied mammals could be more vulnerable to human impacts (Crees *et al.* 2019) and smaller-bodied mammals have experienced an increase in their geographic range (Pacifici *et al.* 2020). Traits 2-7 reflect a set of measurements of growth and reproduction strategies; rapid global changes and human disturbances may favor r-selected strategies that species have high reproduction rates and short lifespan, characteristics commonly associated with invasive species (Bielby *et al.* 2007; Sakai *et al.* 2001). The mammals that hibernate or lower their energy demand (torpor) could boost their chances of survival during extreme conditions, allowing them to withstand climate extremes and habitat degradation in the face of a human-dominated landscape (Geiser & Turbill 2009; Scopes *et al.* 2024). Generalist species that have wider diet and habitat breadth could be more capable of exploiting diverse food resources and habitats, and thus could be more likely to persist or benefit in the context of various human impacts (Pacifici *et al.* 2020; Pineda-Munoz *et al.* 2021). The trophic level of a species could determine the degree of conflicts with humans (Graham *et al.* 2005), while humans also have been exploiting higher trophic levels in both marine and terrestrial environments (Darimont *et al.* 2015). The location and timing of species' activities (e.g. foraging strata, fossoriality, activity cycle, and volant capacity) could affect possible resources that a species could explore, the level of conflict with human disturbances, and a species' capacity to navigate human-modified landscapes (Gaynor *et al.* 2018; Haysom *et al.* 2023; Munguía *et al.* 2016; Pacifici *et al.* 2020).

Statistical analyses

We conducted linear regressions using ordinary least squares (OLS) to investigate the relationship between species' responses to HII and species traits. We used the cumulative sum of the relative probability of presence along the response curve of HII as the response variable and 15 biological traits (6 categorical and 9 numerical) as candidate predictors (Table S3). The adult body mass was log transformed to minimize the difference between extreme large and small values. All the numerical variables were scaled to have a mean of zero and standard deviation of one for easier comparison among their corresponding regression coefficients derived from the OLS models. With all species (219), we performed a stepwise model selection based on the

Akaike information criterion (AIC) to obtain the models with the lowest AIC. In addition, we built stepwise models using OLS for each mammal order to investigate potential differences among their responses to HII; in this case, a predictor would be excluded from a model if all species in that order have the same values for the variable (i.e., no variation present among species). Orders lacking sufficient sample size to allow at least two residual degrees of freedom were not modeled individually, though they remained in the full model. We tested the residuals of all full and stepwise-selected models for phylogenetic signal (Revell 2010). We estimated Pagel's λ for the model residuals across 1,000 phylogenetic trees obtained from PHYLACINE 1.2.1 (Faurby et al. 2018; Faurby et al. 2020) using the 'phytools' R package (Revell 2024). As we found no significant phylogenetic signal (lambda ~ 0; Table S5), we only presented the results of the OLS model.

References:

Bright, E., Coleman, P., Rose, A. & Urban, M. (2011). LandScan Global 2010 [Data set]. *Oak Ridge National Laboratory*.

Crees, J.J., Turvey, S.T., Freeman, R. & Carbone, C. (2019). Mammalian tolerance to humans is predicted by body mass: evidence from long-term archives. *Ecology*, 100, e02783.

Darimont, C.T., Fox, C.H., Bryan, H.M. & Reimchen, T.E. (2015). The unique ecology of human predators. *Science*, 349, 858–860.

Elith, J., Leathwick, J.R. & Hastie, T. (2008). A working guide to boosted regression trees. *J. Anim. Ecol.*, 77, 802–813.

Elvidge, C.D., Zhizhin, M., Ghosh, T., Hsu, F.-C. & Taneja, J. (2021). Annual time series of global VIIRS nighttime lights derived from monthly averages: 2012 to 2019. *Remote Sens.*, 13, 922.

Fahrig, L. & Rytwinski, T. (2009). Effects of Roads on Animal Abundance: an Empirical Review and Synthesis. *Ecol. Soc.*, 14.

Geiser, F. & Turbill, C. (2009). Hibernation and daily torpor minimize mammalian extinctions. *Naturwissenschaften*, 96, 1235–1240.

Graham, K., Beckerman, A.P. & Thirgood, S. (2005). Human–predator–prey conflicts: ecological correlates, prey losses and patterns of management. *Biol. Conserv.*, 122, 159–171.

Haysom, J.K., Deere, N.J., Mahyudin, A. & Struebig, M.J. (2023). Stratified activity: Vertical partitioning of the diel cycle by rainforest mammals in Borneo. *Biotropica*, 55, 991–1005.

Hijmans, R.J., Phillips, S., Leathwick, J., Elith, J. & Hijmans, M.R.J. (2017). Package "dismo." *Circles*, 9, 1–68.

Hirzel, A.H., Le Lay, G., Helfer, V., Randin, C. & Guisan, A. (2006). Evaluating the ability of habitat suitability models to predict species presences. *Ecol. Modell.*, 199, 142–152.

IUCN. (2022). *The IUCN Red List of Threatened Species. 2022-1*. Available at: https://www.iucnredlist.org/. Last accessed December 2022.

Meijer, J.R., Huijbregts, M.A.J., Schotten, K.C.G.J. & Schipper, A.M. (2018). Global patterns of current and future road infrastructure. *Environ. Res. Lett.*, 13, 064006.

Munguía, M., Trejo, I., González-Salazar, C. & Pérez-Maqueo, O. (2016). Human impact gradient on mammalian biodiversity. *Global Ecology and Conservation*, 6, 79–92.

Papeş, M. & Gaubert, P. (2007). Modelling ecological niches from low numbers of occurrences: assessment of the conservation status of poorly known viverrids (Mammalia, Carnivora) across two continents. *Divers. Distrib.*, 13, 890–902.
Peterson, A.T., Papeş, M. & Soberón, J. (2008). Rethinking receiver operating characteristic analysis applications in ecological niche modeling. *Ecol. Modell.*, 213, 63–72.
Phillips, S.J., Dudík, M. & Schapire, R.E. (2004). A maximum entropy approach to species distribution modeling. In: *Proceedings of the twenty-first international conference on Machine learning*. ACM, p. 83.
Pyšek, P., Jarošík, V., Hulme, P.E., Kühn, I., Wild, J., Arianoutsou, M., *et al.* (2010). Disentangling the role of environmental and human pressures on biological invasions across Europe. *Proc. Natl. Acad. Sci. U.S.A.*, 107, 12157–12162.
Ramankutty, N., Evan, A.T., Monfreda, C. & Foley, J.A. (2010a). Global Agricultural Lands: Croplands, 2000.
Ramankutty, N., Evan, A.T., Monfreda, C. & Foley, J.A. (2010b). Global Agricultural Lands: Pastures, 2000.
R Core Team. (2024). *R: A Language and Environment for Statistical Computing*. R Foundation for Statistical Computing, Vienna, Austria.
Scopes, E.R., Broome, A., Walsh, K., Bennie, J.J. & McDonald, R.A. (2024). Conservation implications of hibernation in mammals. *Mamm. Rev.*, 54, 310–324.
Shilereyo, M.T., Magige, F.J., Ogutu, J.O. & Røskaft, E. (2023). Small-mammal abundance and species diversity: land use and seasonal influences in the Serengeti Ecosystem, Tanzania. *Front. Conserv. Sci.*, 4.
Swets, J.A. (1979). ROC analysis applied to the evaluation of medical imaging techniques. *Invest. Radiol.*, 14, 109–121.

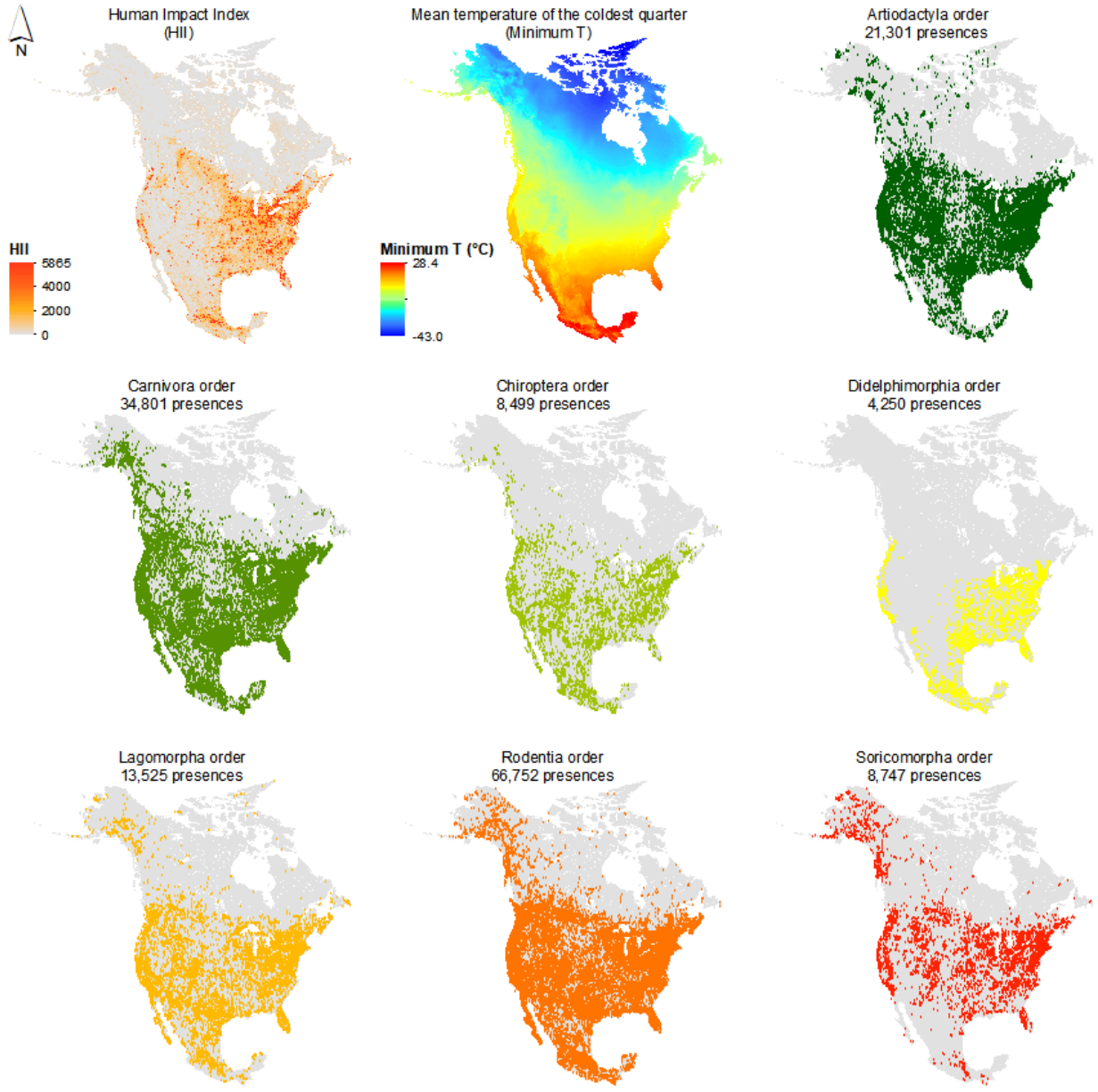

Figure S1. Spatial distributions of human impact index (HII), mean temperature of the coldest quarter (Minimum T), and filtered species presences (157,875 records) across seven mammal orders in North America.

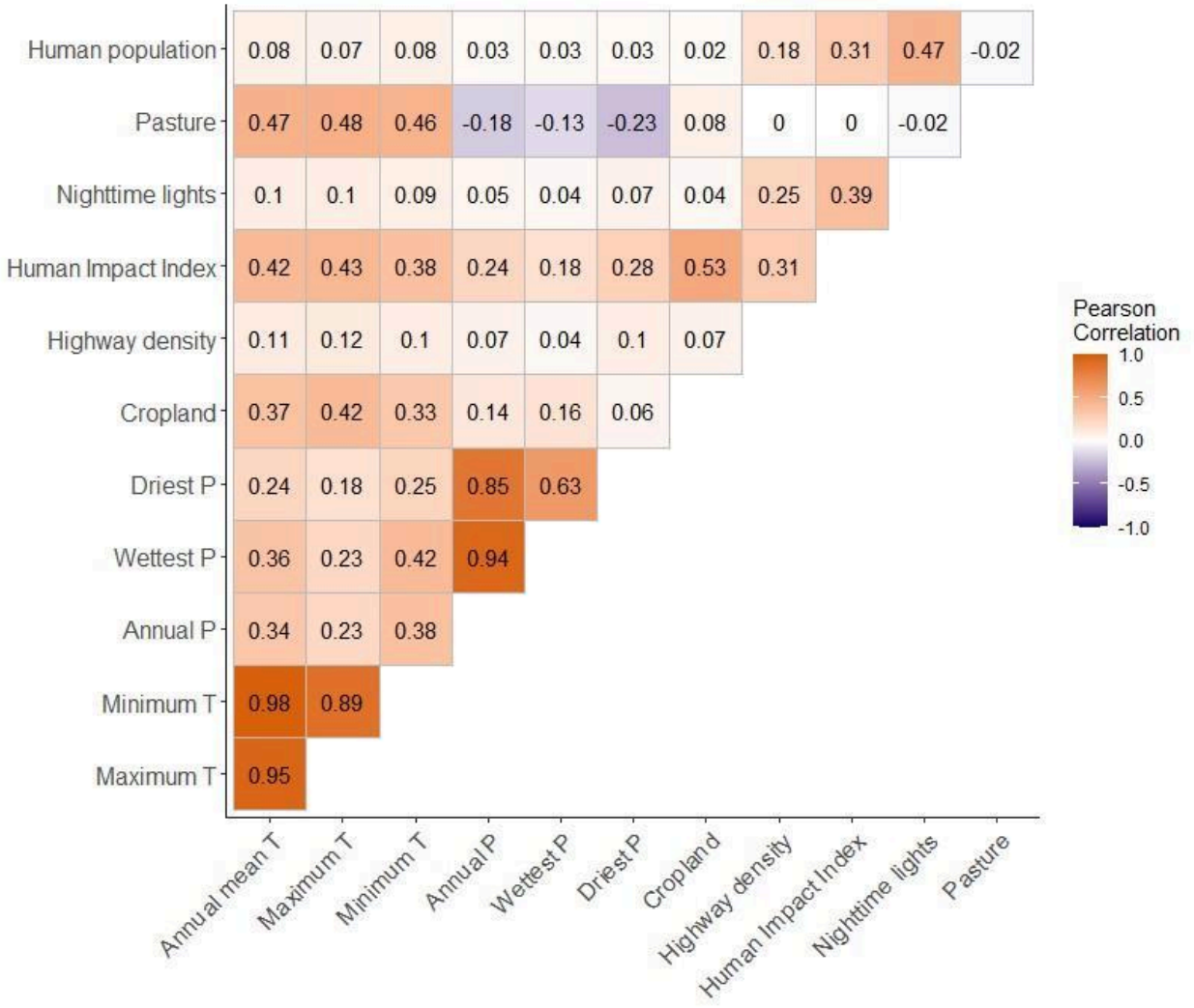

Figure S2. Correlation matrix of Pearson correlation coefficients for the 12 selected anthropogenic and climatic factors. Warm colors indicate positive correlations, while cold colors represent negative correlations. White colors mean no correlation.

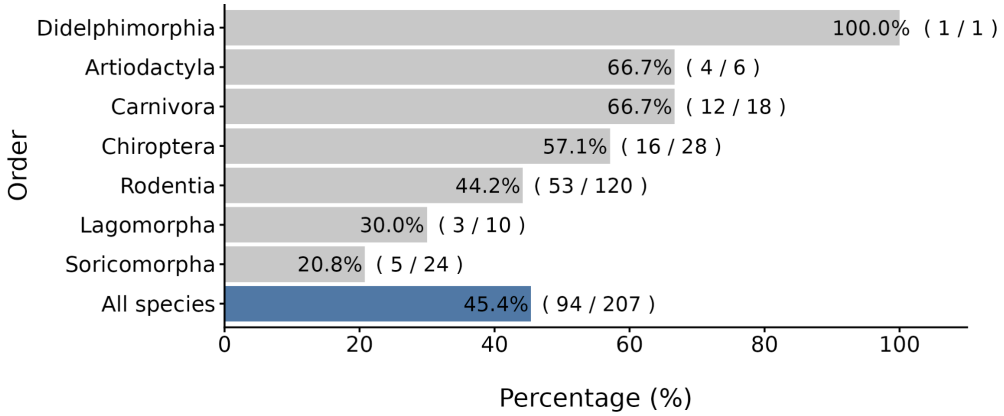

Figure S3. The percentage of species within each mammal order that has an anthropogenic factor ranked as the top contributing variable for the models fit with Maxent but with all human observations excluded.

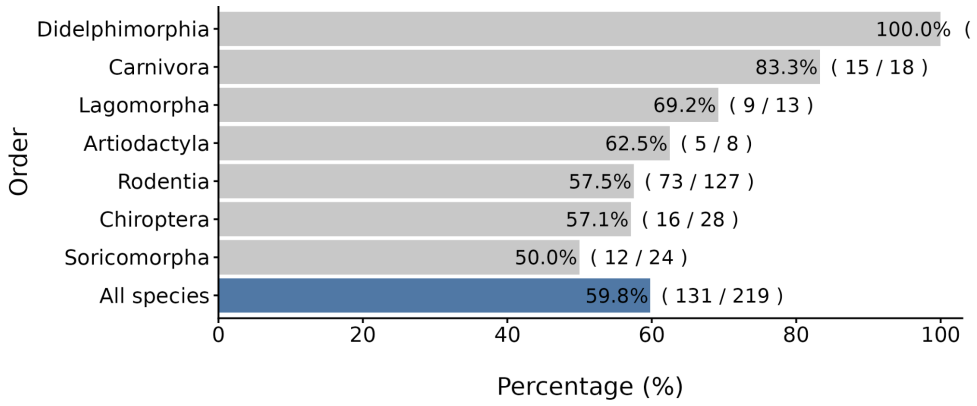

Figure S4. The percentage of species within each mammal order that has an anthropogenic factor ranked as the top contributing variable for the models fit with the BRT algorithm.

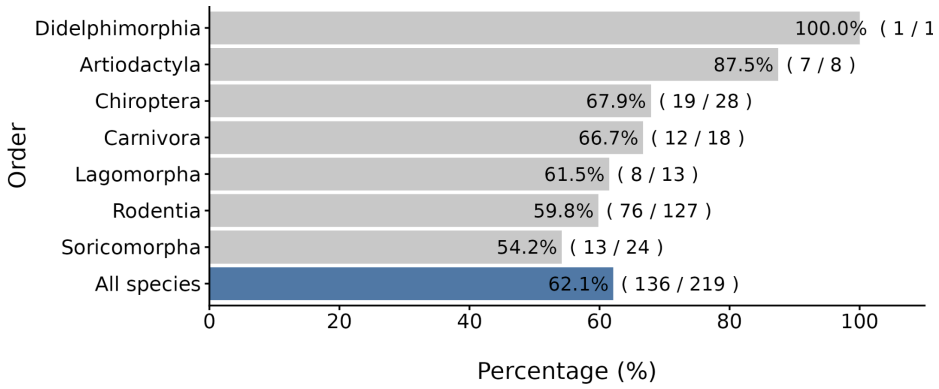

Figure S5. The percentage of species within each mammal order that has an anthropogenic factor ranked as the top contributing variable for the models fit with the 6 anthropogenic factors and 6 bioclimatic principal components (PCs).

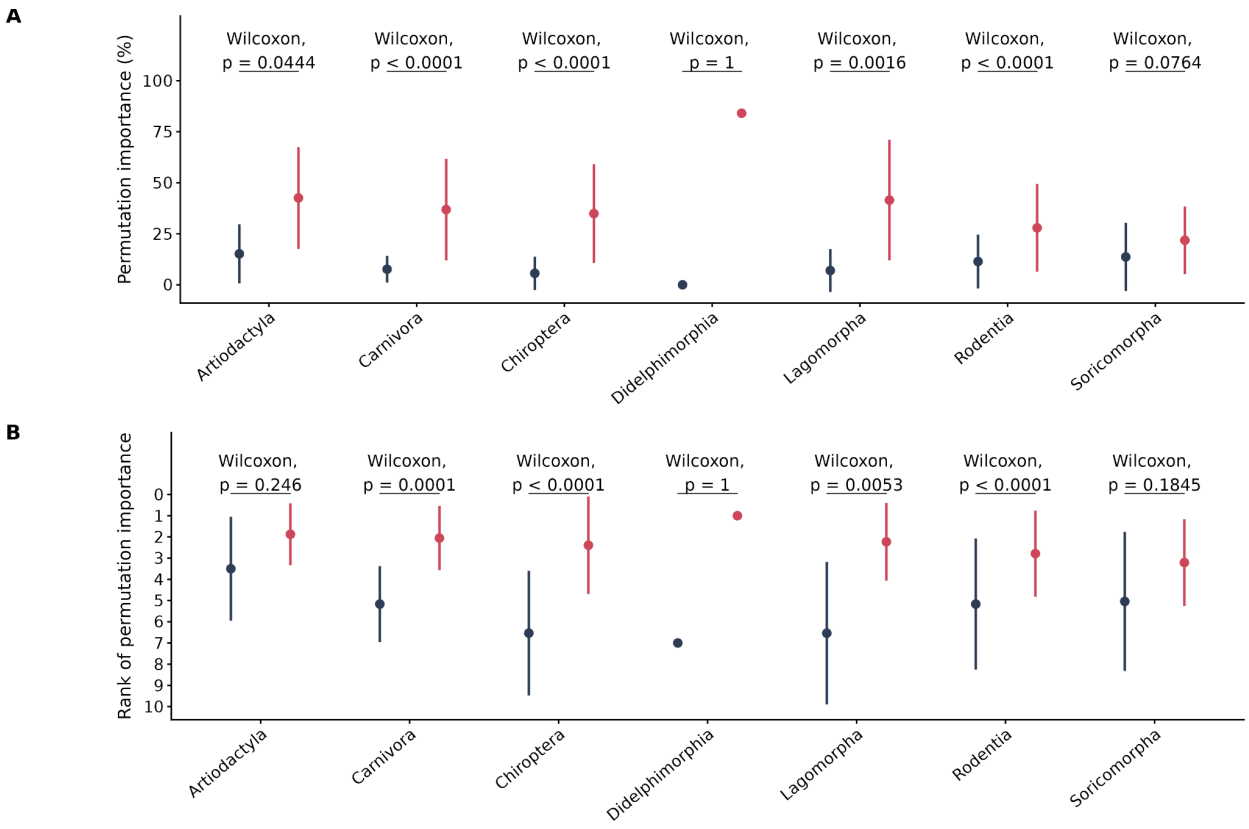

Figure S6. Comparison of variable importance between human impact index (HII) and mean temperature of the warmest quarter (Maximum T) for each order. The figure shows the results of comparing variable importance (A) and rank of variable importance (B) between HII and Maximum T for each order using the Wilcoxon signed-rank test (Wilcoxon) with a Hommel correction for multiple hypothesis testing. HII was colored in red, and Maximum T was colored in blue. The p-values greater than 0.05 indicated non-significant results, while those less than 0.05 indicated significant differences.

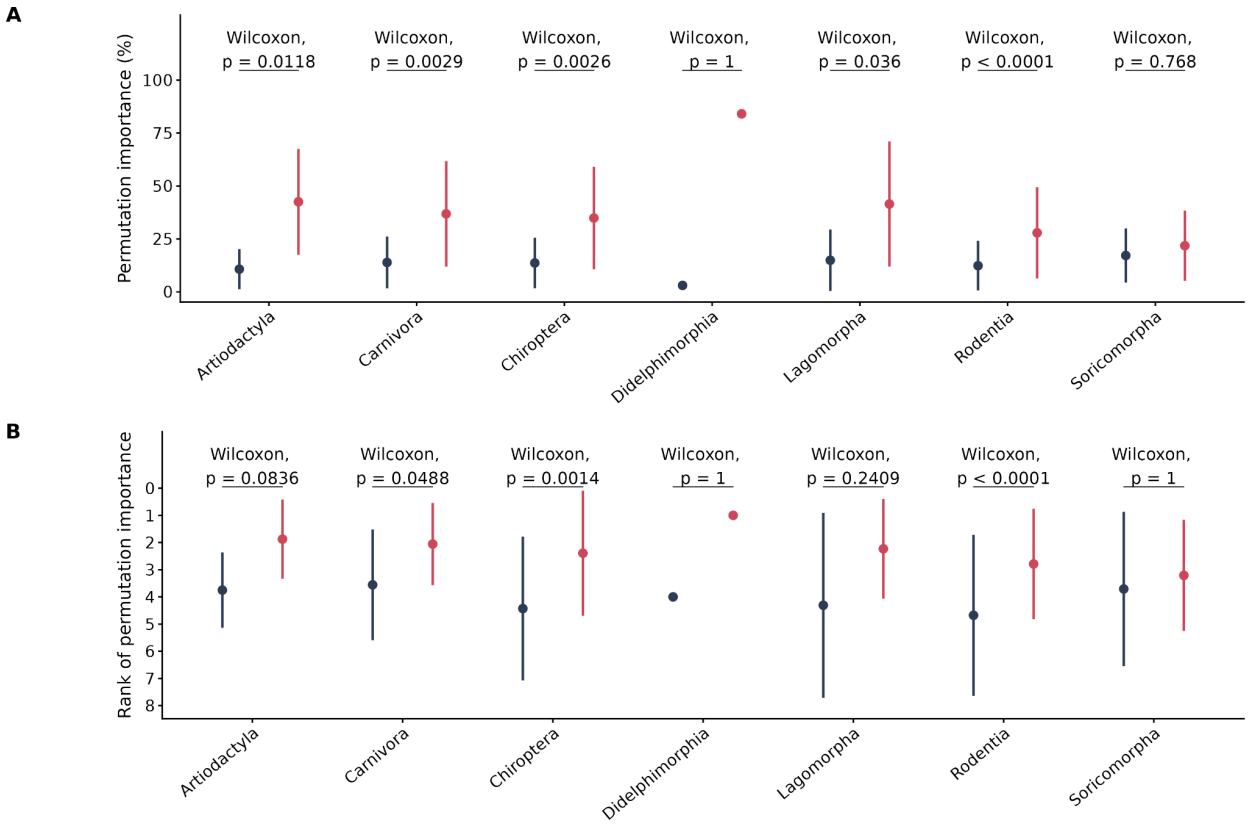

Figure S7. Comparison of variable importance between human impact index (HII) and mean temperature of coldest quarter (Minimum T) for each order. The figure shows the results of comparing variable importance (A) and rank of variable importance (B) between HII and Minimum T for each order using the Wilcoxon signed-rank test (Wilcoxon) with a Hommel correction for multiple hypothesis testing. HII was colored in red, and Minimum T was colored in blue. The p-values greater than 0.05 indicated non-significant results, while those less than 0.05 indicated significant differences.

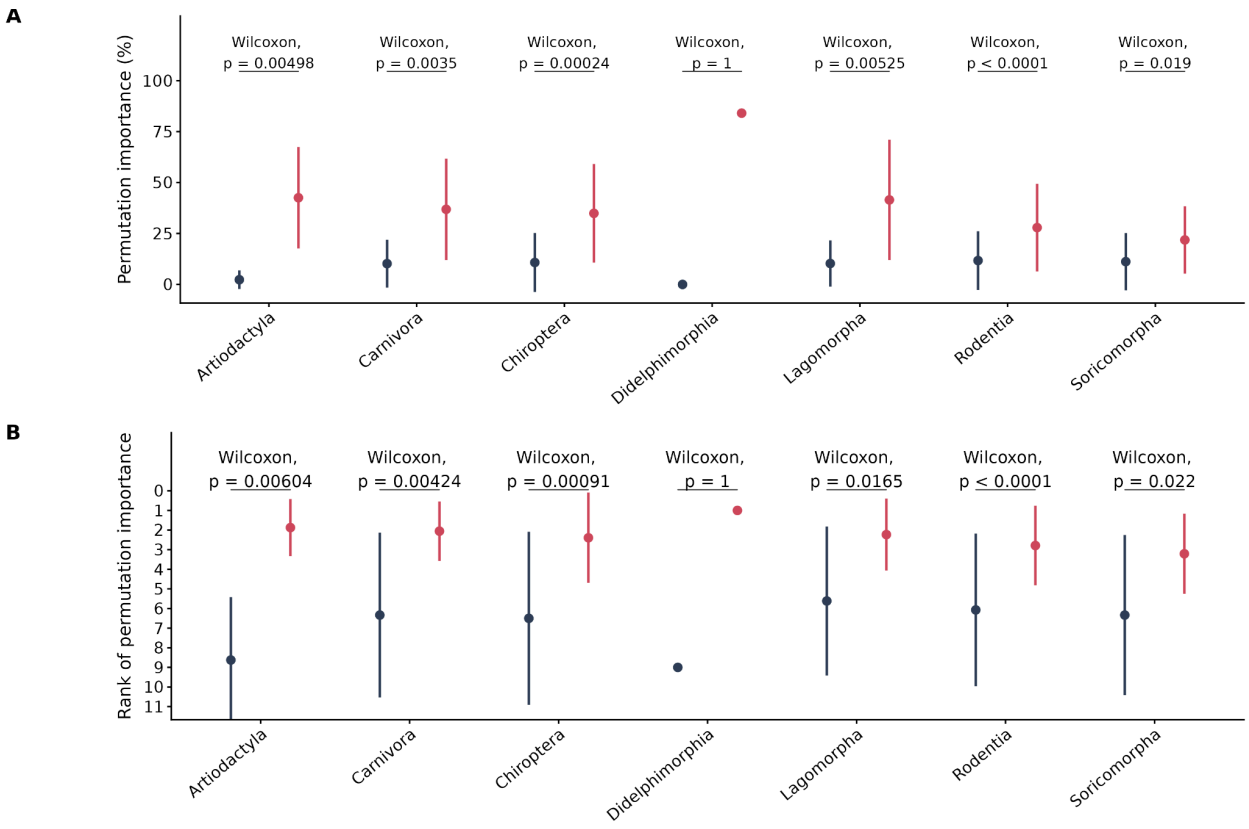

Figure S8. Comparison of variable importance between human impact index (HII) and annual mean temperature (Annual mean T) for each order. The figure shows the results of comparing variable importance (A) and rank of variable importance (B) between HII and Annual mean T for each order using the Wilcoxon signed-rank test (Wilcoxon) with a Hommel correction for multiple hypothesis testing. HII was colored in red, and bio1 was colored in blue. The p-values greater than 0.05 indicated non-significant results, while those less than 0.05 indicated significant differences.

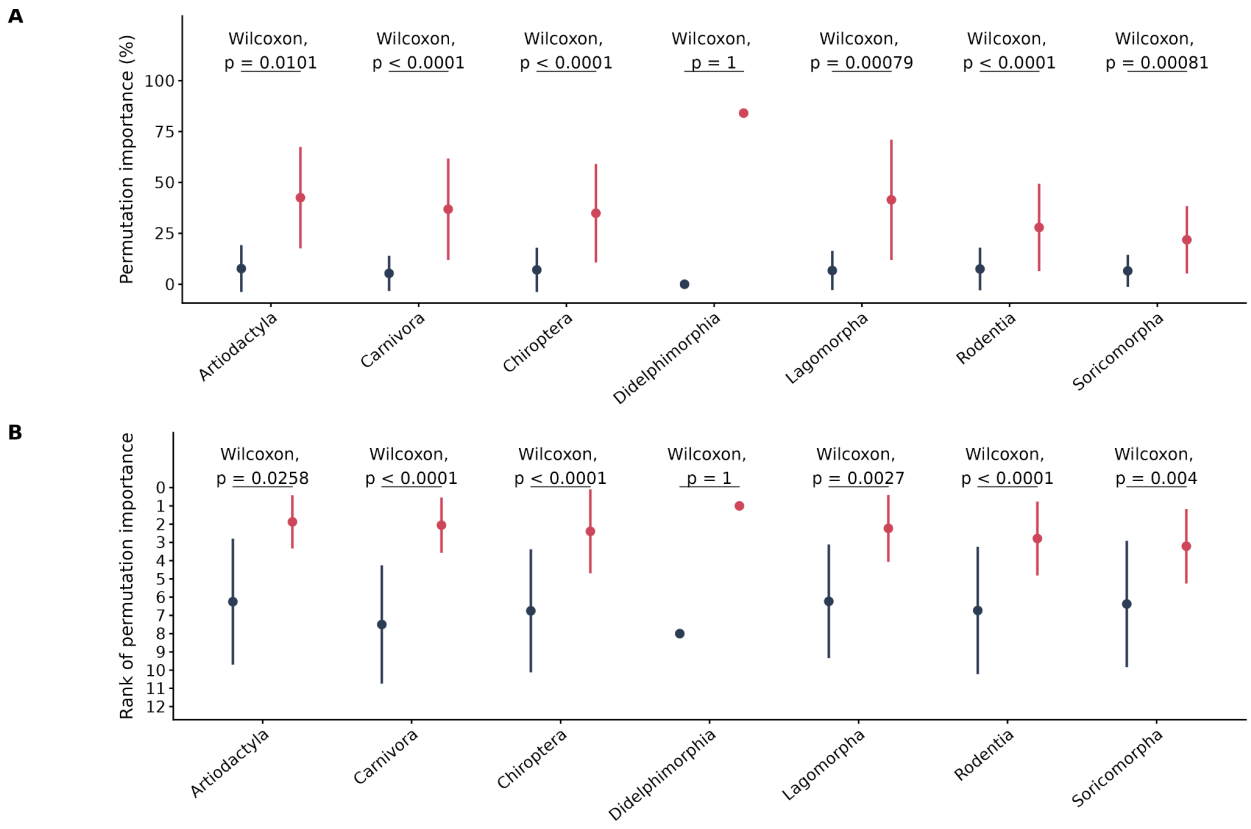

Figure S9. Comparison of variable importance between human impact index (HII) and annual precipitation (Annual P) for each order. The figure shows the results of comparing variable importance (A) and rank of variable importance (B) between HII and Annual P for each order using the Wilcoxon signed-rank test (Wilcoxon) with a Hommel correction for multiple hypothesis testing. HII was colored in red, and Annual P was colored in blue. The p-values greater than 0.05 indicated non-significant results, while those less than 0.05 indicated significant differences.

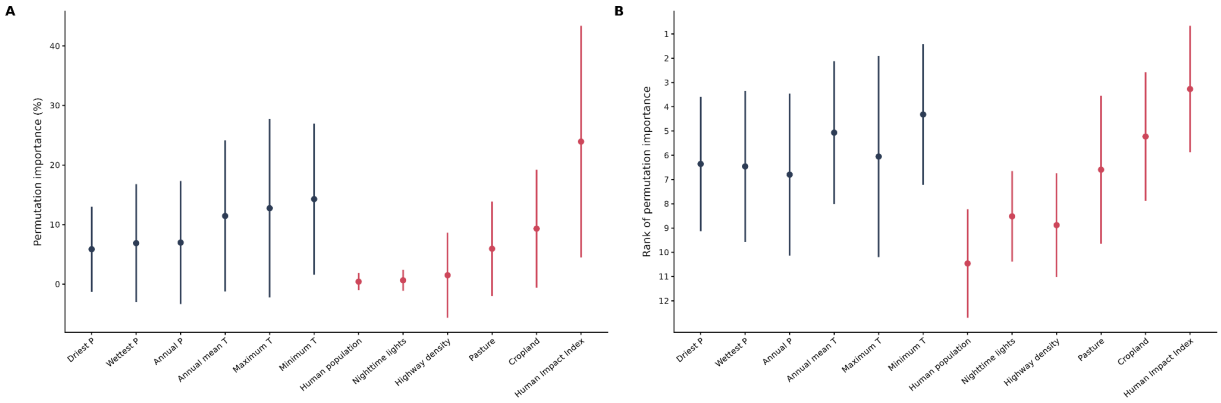

Figure S10. Variable importance of each predictor for the model fit with Maxent but with all human observations excluded. Panel A shows the variable importance, and panel B shows the rank of variable importance for each predictor variable. Climatic variables are colored as blue, and anthropogenic variables are colored as red. The error bars represent the one SD around the means.

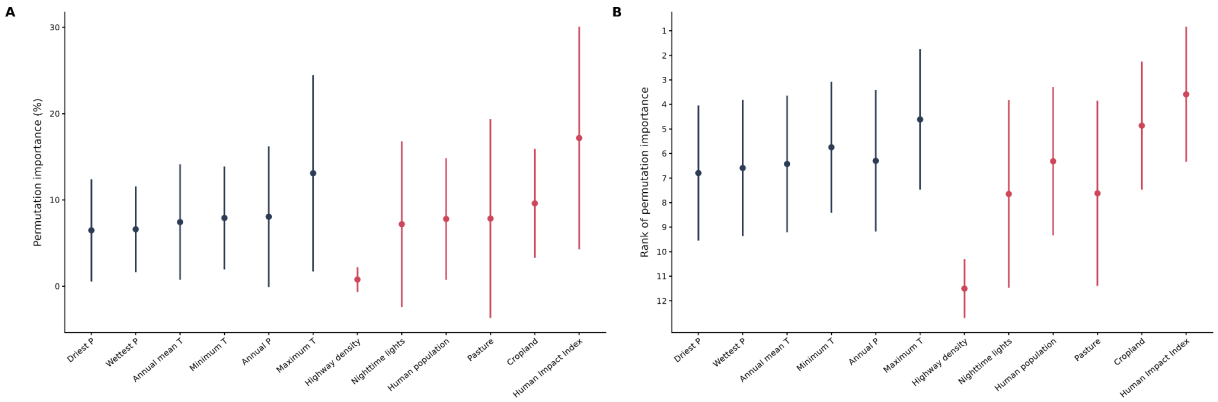

Figure S11. Variable importance of each predictor for the model fit with the BRT algorithm. Panel A shows the variable importance, and panel B shows the rank of variable importance for each predictor variable. Climatic variables are colored as blue, and anthropogenic factors are colored as red. The error bars represent the one SD around the means.

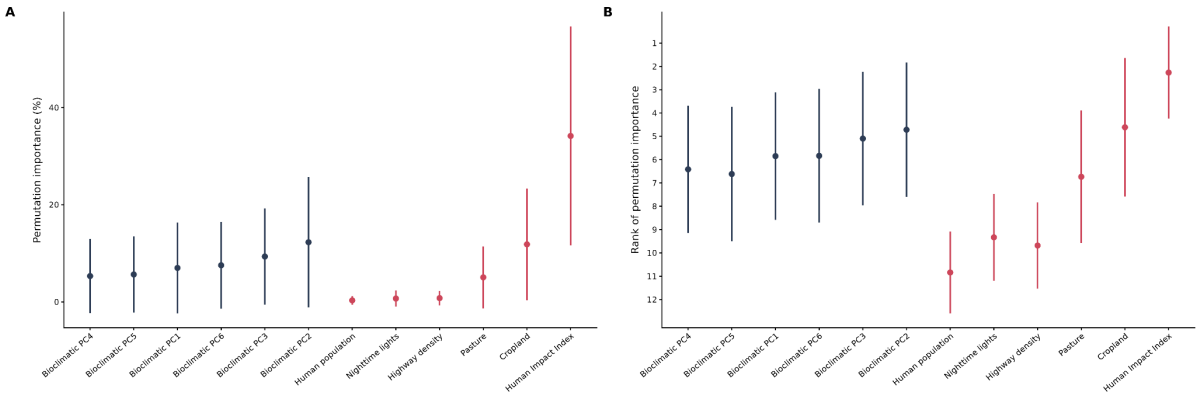

Figure S12. Variable importance of each predictor for the model fit with 6 anthropogenic factors and 6 bioclimatic principal components. Panel A shows the variable importance, and panel B shows the rank of variable importance for each predictor variable. Climatic variables are colored as blue, and anthropogenic factors are colored as red. The error bars represent the one SD around the means.

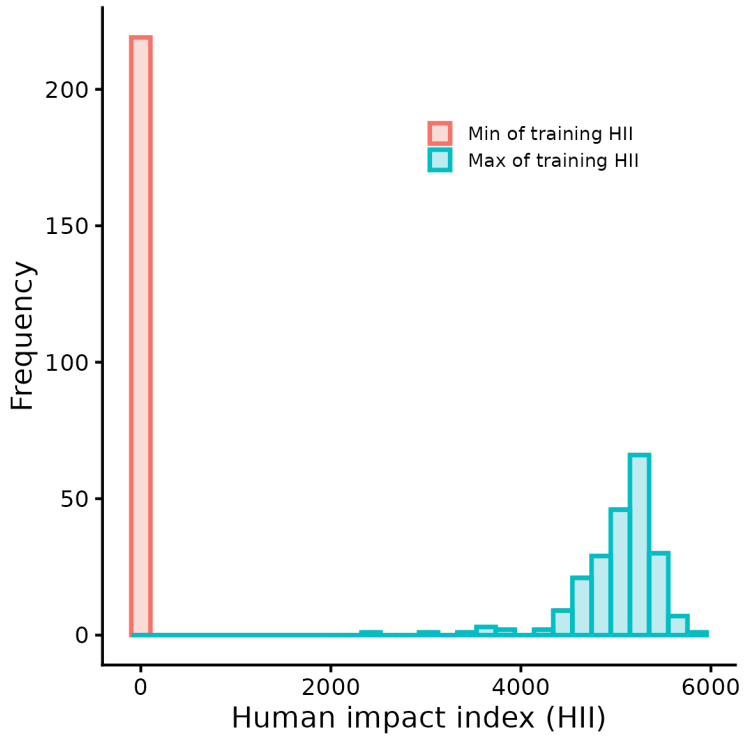

Figure S13. Histogram of the minimum and maximum human impact index (HII) values for species investigated (n = 219). The HII values in the study area range from 0 to 5865.

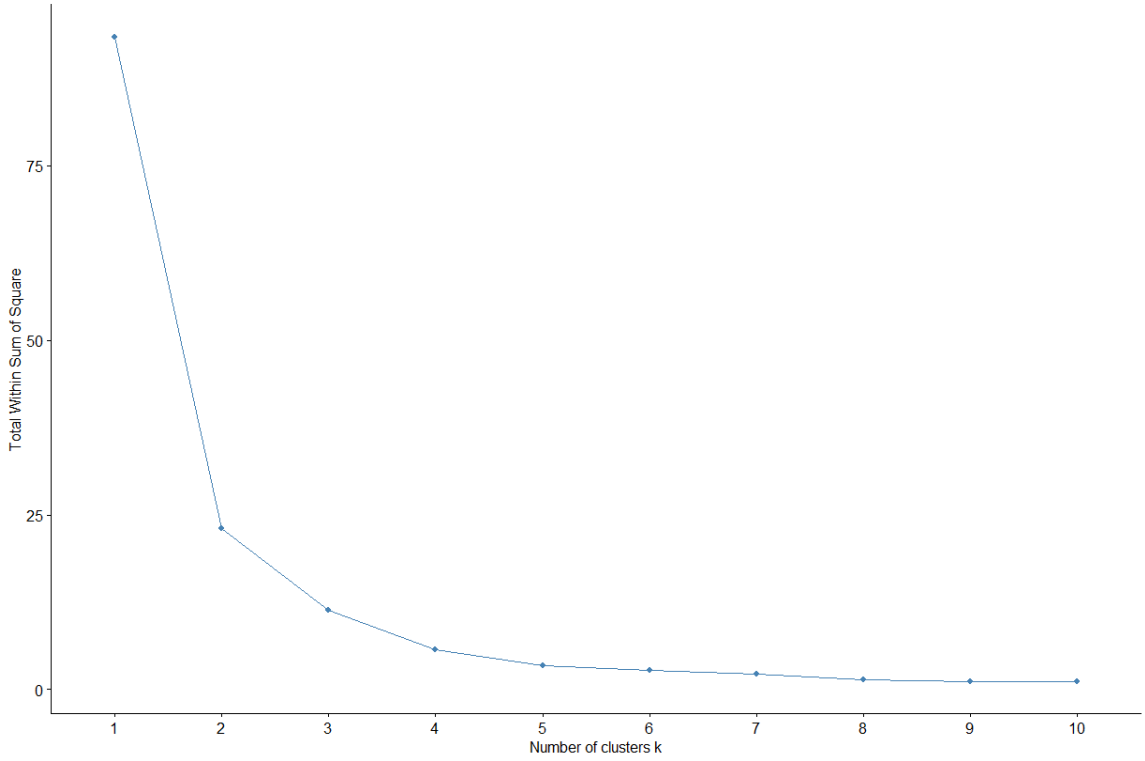

Figure S14. Optimal number of clusters for HII response-curve grouping. The elbow plot shows the total within-cluster sum of squares from k-means clustering of the response-curve index across candidate values of k. The sharp decline from k = 1 to k = 4, followed by a smaller reduction after k = 5, indicates that five clusters provide a reasonable explanation for variation in response-curve structure and avoid over-partitioning.

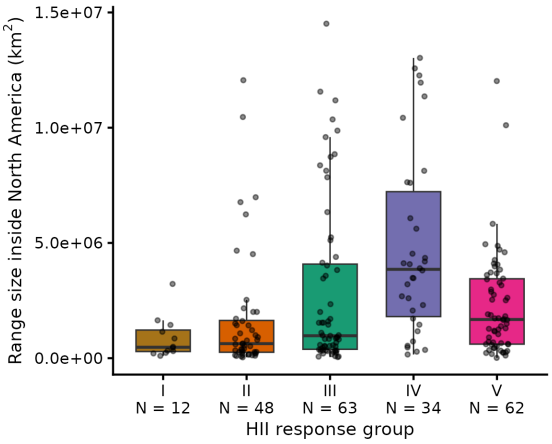

Figure S15. Boxplot of species range size among five groups of species. The grouping of species is based on their responses to the human impact index (see Methods).

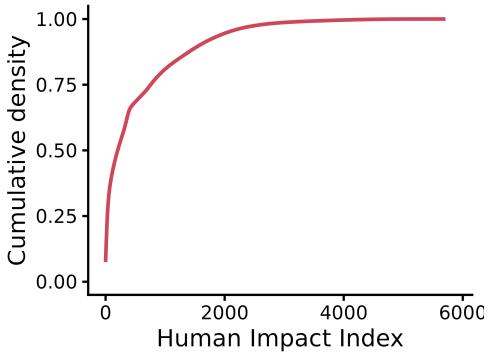

Figure S16. Cumulative density of human impact index (HII) values in North America. HII < 2000 corresponds to 95% of the areas, and HII > 5000 corresponds to 0.01% of the areas.

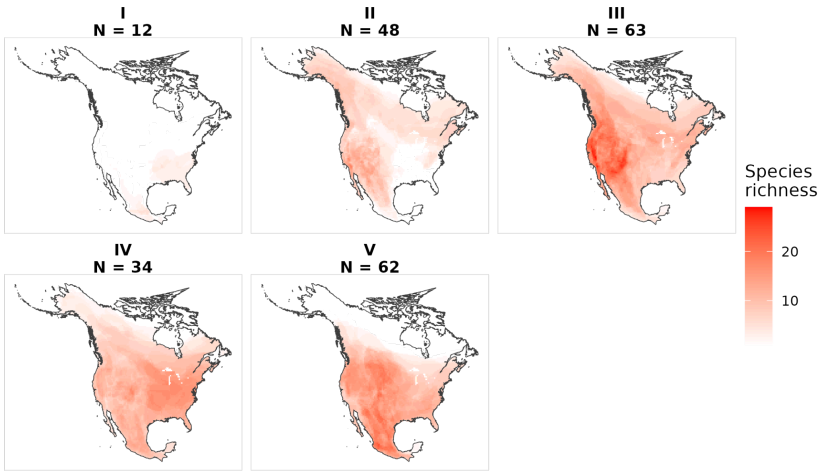

Figure S17. Richness maps of the five groups of species. The grouping of species is based on their responses to the human impact index (see Methods).

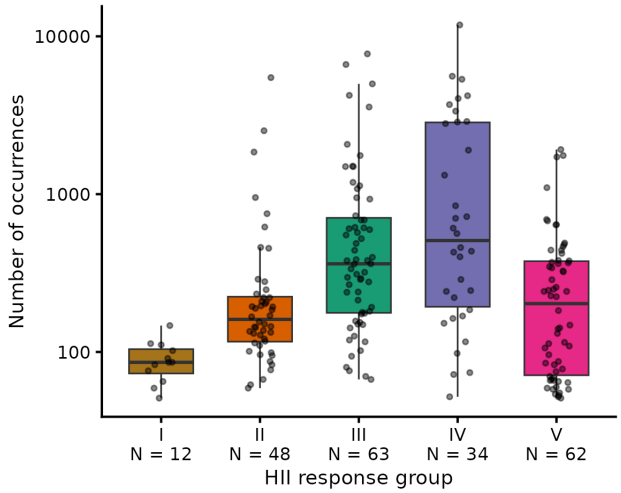

Figure S18. Boxplot of species occurrence size among five groups of species. The grouping of species is based on their responses to the human impact index (see Methods).

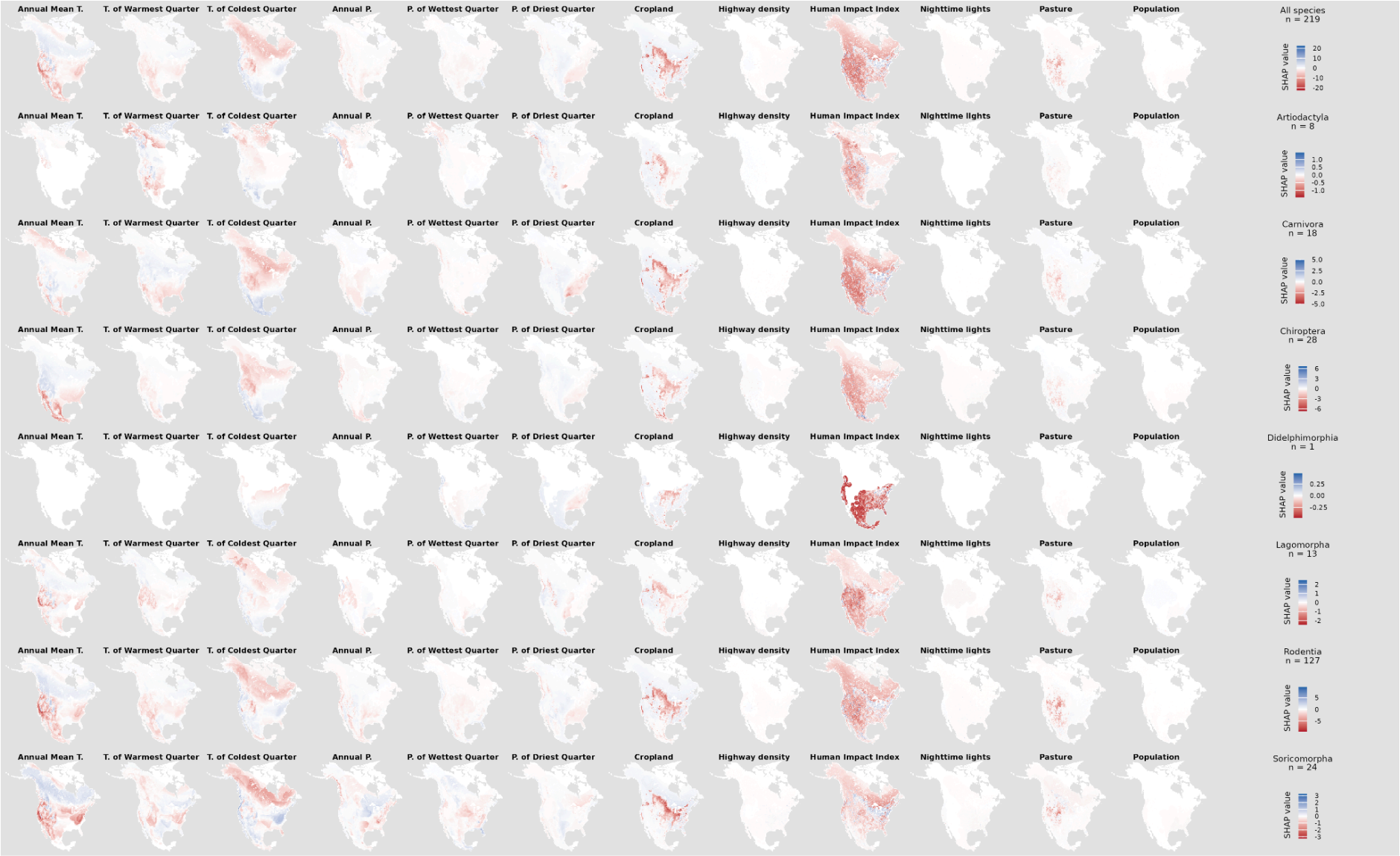

Figure S19. Aggregated SHAP maps for 12 environmental factors. SHAP values are aggregated across all species (n = 219) and separately within each mammal order. Blue indicates positive SHAP values, red indicates negative SHAP values, and white indicates zero.

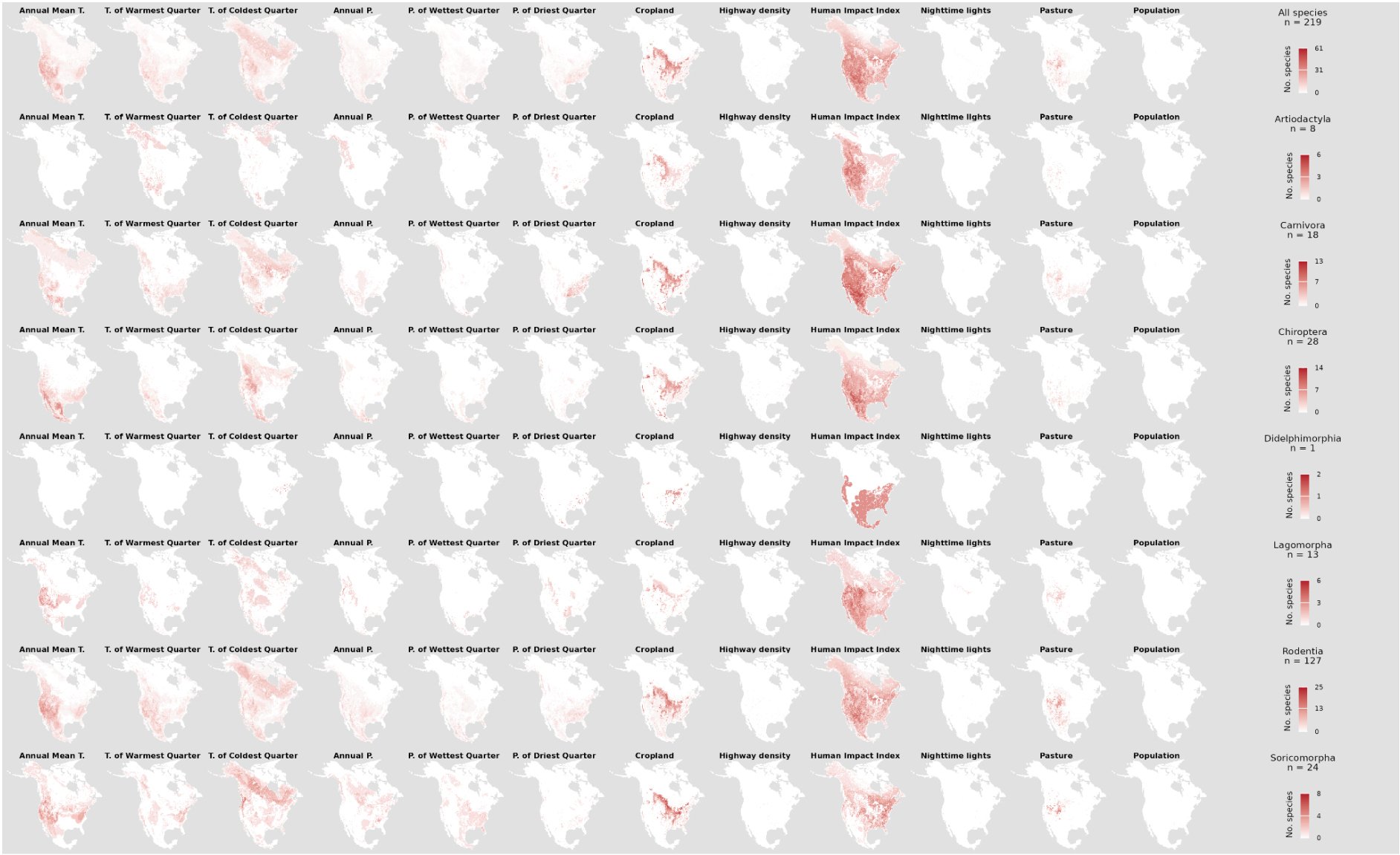

Figure S20. Frequency maps of locally dominating effects for 12 environmental factors. For each species and raster cell, the factor with the largest absolute SHAP value is identified as the locally dominant factor. Maps show the number of species for which each factor is locally dominant, summarized across all species (n = 219) and separately within each mammal order. Darker red indicates a larger number of species for which that factor is the dominant factor.

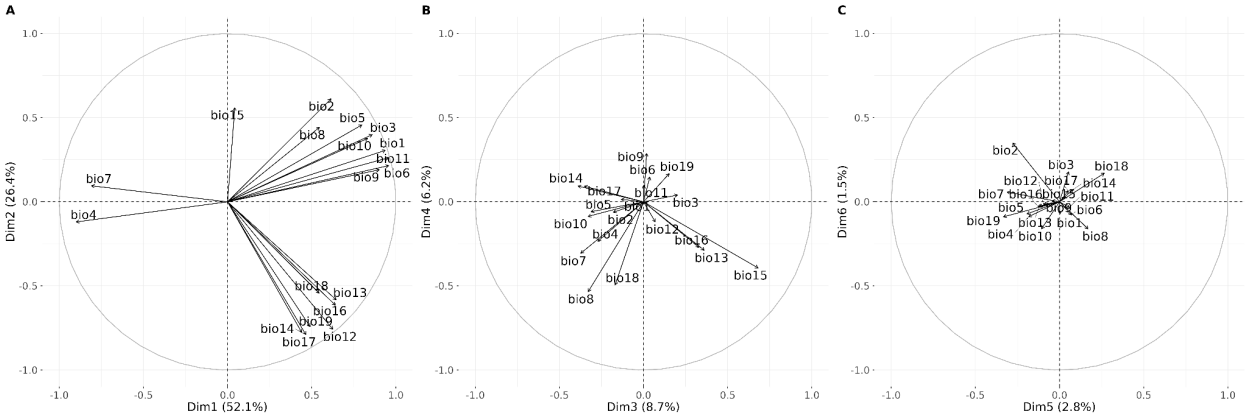

Figure S21. Plots showing the relationships between the original 19 bioclimatic variables and the first six principal components (PC) used in Maxent modeling. Arrows indicate the direction and strength of each bioclimatic variable's loading on a pair of principal components (PC1-PC2, PC3-PC4, and PC5-PC6). Axis labels show the percentage of variation explained by each PC.

Table S1. Species and order name, number of spatially unique presences, and Maxent model evaluation indices derived from testing data, which include the mean and standard deviation of the area under the receiver operating characteristic curve (AUC) and continuous Boyce index (CBI).

Order	Scientific name	Number of spatially unique presences	AUC (sd)	CBI (sd)
Artiodactyla	*Antilocapra americana*	1,848	0.70 (0.01)	0.94 (0.05)
Artiodactyla	*Bison bison*	221	0.84 (0.02)	0.91 (0.04)
Artiodactyla	*Odocoileus hemionus*	4,999	0.73 (0.01)	0.90 (0.03)
Artiodactyla	*Odocoileus virginianus*	11,810	0.67 (0.01)	0.92 (0.03)
Artiodactyla	*Oreamnos americanus*	460	0.72 (0.03)	0.93 (0.05)
Artiodactyla	*Ovibos moschatus*	152	0.74 (0.04)	0.83 (0.06)
Artiodactyla	*Ovis canadensis*	1,495	0.63 (0.02)	0.82 (0.06)
Artiodactyla	*Ovis dalli*	297	0.77 (0.04)	0.93 (0.01)
Carnivora	*Bassariscus astutus*	703	0.75 (0.02)	0.98 (0.01)
Carnivora	*Canis latrans*	6,629	0.73 (0.01)	0.96 (0.02)
Carnivora	*Conepatus leuconotus*	487	0.62 (0.03)	0.81 (0.11)
Carnivora	*Lynx canadensis*	551	0.78 (0.01)	0.96 (0.01)
Carnivora	*Lynx rufus*	3,565	0.73 (0.01)	0.99 (0.01)
Carnivora	*Martes americana*	609	0.76 (0.02)	0.95 (0.03)
Carnivora	*Martes pennanti*	322	0.75 (0.05)	0.85 (0.09)
Carnivora	*Mephitis macroura*	267	0.68 (0.03)	0.74 (0.10)
Carnivora	*Mephitis mephitis*	3,356	0.79 (0.01)	0.98 (0.01)
Carnivora	*Mustela frenata*	288	0.77 (0.03)	0.91 (0.04)
Carnivora	*Procyon lotor*	7,741	0.75 (0.00)	0.98 (0.03)

Carnivora	*Spilogale gracilis*	240	0.75 (0.04)	0.88 (0.07)
Carnivora	*Spilogale putorius*	148	0.63 (0.03)	0.57 (0.21)
Carnivora	*Taxidea taxus*	1,130	0.69 (0.01)	0.93 (0.02)
Carnivora	*Urocyon cinereoargenteus*	2,865	0.76 (0.01)	0.99 (0.01)
Carnivora	*Ursus americanus*	5,476	0.74 (0.01)	0.99 (0.01)
Carnivora	*Vulpes macrotis*	289	0.69 (0.03)	0.84 (0.12)
Carnivora	*Vulpes velox*	113	0.61 (0.05)	0.48 (0.17)
Chiroptera	*Antrozous pallidus*	479	0.69 (0.03)	0.90 (0.05)
Chiroptera	*Balantiopteryx plicata*	131	0.83 (0.04)	0.81 (0.11)
Chiroptera	*Choeronycteris mexicana*	142	0.75 (0.06)	0.83 (0.05)
Chiroptera	*Corynorhinus townsendii*	347	0.69 (0.02)	0.85 (0.03)
Chiroptera	*Dermanura azteca*	64	0.70 (0.10)	0.79 (0.11)
Chiroptera	*Eptesicus fuscus*	1,720	0.80 (0.02)	0.99 (0.00)
Chiroptera	*Glossophaga morenoi*	76	0.70 (0.05)	0.71 (0.10)
Chiroptera	*Lasionycteris noctivagans*	490	0.79 (0.04)	0.94 (0.03)
Chiroptera	*Lasiurus borealis*	677	0.72 (0.02)	0.95 (0.03)
Chiroptera	*Lasiurus intermedius*	59	0.78 (0.08)	0.90 (0.04)
Chiroptera	*Lasiurus seminolus*	66	0.79 (0.09)	0.91 (0.07)
Chiroptera	*Lasiurus xanthinus*	65	0.72 (0.04)	0.86 (0.09)
Chiroptera	*Leptonycteris yerbabuenae*	169	0.74 (0.03)	0.87 (0.05)
Chiroptera	*Macrotus californicus*	77	0.66 (0.06)	0.68 (0.13)
Chiroptera	*Myotis californicus*	442	0.75 (0.02)	0.95 (0.02)

Chiroptera	*Myotis ciliolabrum*	83	0.81 (0.06)	0.92 (0.04)
Chiroptera	*Myotis evotis*	242	0.76 (0.04)	0.87 (0.06)
Chiroptera	*Myotis lucifugus*	563	0.84 (0.01)	0.94 (0.04)
Chiroptera	*Myotis occultus*	70	0.82 (0.06)	0.85 (0.08)
Chiroptera	*Myotis septentrionalis*	52	0.66 (0.12)	0.60 (0.29)
Chiroptera	*Myotis thysanodes*	185	0.66 (0.04)	0.76 (0.12)
Chiroptera	*Myotis velifer*	257	0.66 (0.05)	0.83 (0.09)
Chiroptera	*Myotis volans*	242	0.73 (0.03)	0.90 (0.03)
Chiroptera	*Myotis yumanensis*	363	0.80 (0.04)	0.91 (0.03)
Chiroptera	*Nycticeius humeralis*	227	0.72 (0.03)	0.87 (0.05)
Chiroptera	*Nyctinomops femorosaccus*	54	0.68 (0.06)	0.73 (0.10)
Chiroptera	*Parastrellus hesperus*	242	0.69 (0.05)	0.74 (0.29)
Chiroptera	*Perimyotis subflavus*	380	0.66 (0.01)	0.87 (0.09)
Didelphimorphia	*Didelphis virginiana*	4,204	0.77 (0.01)	0.99 (0.00)
Lagomorpha	*Lepus alleni*	126	0.66 (0.05)	0.63 (0.28)
Lagomorpha	*Lepus americanus*	1,504	0.78 (0.01)	0.99 (0.00)
Lagomorpha	*Lepus californicus*	2,068	0.69 (0.01)	0.96 (0.03)
Lagomorpha	*Lepus townsendii*	287	0.75 (0.03)	0.89 (0.05)
Lagomorpha	*Ochotona collaris*	128	0.79 (0.05)	0.82 (0.07)
Lagomorpha	*Ochotona princeps*	686	0.87 (0.01)	0.97 (0.02)
Lagomorpha	*Sylvilagus aquaticus*	174	0.72 (0.04)	0.78 (0.12)
Lagomorpha	*Sylvilagus audubonii*	1,757	0.77 (0.02)	0.99 (0.01)

Lagomorpha	*Sylvilagus bachmani*	336	0.82 (0.02)	0.93 (0.04)
Lagomorpha	*Sylvilagus cunicularius*	66	0.68 (0.07)	0.52 (0.32)
Lagomorpha	*Sylvilagus floridanus*	5,586	0.78 (0.01)	0.99 (0.01)
Lagomorpha	*Sylvilagus nuttallii*	435	0.78 (0.04)	0.90 (0.07)
Lagomorpha	*Sylvilagus palustris*	221	0.77 (0.03)	0.90 (0.04)
Rodentia	*Ammospermophilus harrisii*	178	0.76 (0.05)	0.85 (0.03)
Rodentia	*Ammospermophilus interpres*	53	0.64 (0.14)	0.67 (0.30)
Rodentia	*Ammospermophilus leucurus*	604	0.71 (0.02)	0.94 (0.02)
Rodentia	*Aplodontia rufa*	67	0.67 (0.09)	0.72 (0.10)
Rodentia	*Baiomys musculus*	96	0.68 (0.06)	0.63 (0.17)
Rodentia	*Baiomys taylori*	246	0.64 (0.02)	0.71 (0.28)
Rodentia	*Callospermophilus lateralis*	1,188	0.82 (0.01)	0.99 (0.01)
Rodentia	*Callospermophilus saturatus*	87	0.66 (0.04)	0.58 (0.18)
Rodentia	*Chaetodipus arenarius*	116	0.75 (0.04)	0.87 (0.04)
Rodentia	*Chaetodipus californicus*	131	0.67 (0.06)	0.69 (0.16)
Rodentia	*Chaetodipus eremicus*	74	0.63 (0.07)	0.53 (0.32)
Rodentia	*Chaetodipus fallax*	80	0.67 (0.06)	0.71 (0.19)
Rodentia	*Chaetodipus intermedius*	157	0.62 (0.03)	0.71 (0.12)
Rodentia	*Chaetodipus nelsoni*	142	0.65 (0.05)	0.49 (0.27)
Rodentia	*Chaetodipus penicillatus*	150	0.66 (0.06)	0.69 (0.16)
Rodentia	*Chaetodipus spinatus*	137	0.66 (0.07)	0.62 (0.24)
Rodentia	*Clethrionomys gapperi*	320	0.75 (0.02)	0.90 (0.07)

Rodentia	*Cratogeomys castanops*	115	0.69 (0.04)	0.77 (0.09)
Rodentia	*Cynomys gunnisoni*	176	0.77 (0.04)	0.83 (0.05)
Rodentia	*Cynomys leucurus*	101	0.82 (0.06)	0.87 (0.09)
Rodentia	*Cynomys ludovicianus*	465	0.72 (0.04)	0.91 (0.04)
Rodentia	*Cynomys mexicanus*	70	0.71 (0.05)	0.72 (0.13)
Rodentia	*Dipodomys agilis*	62	0.73 (0.04)	0.74 (0.08)
Rodentia	*Dipodomys deserti*	111	0.64 (0.04)	0.61 (0.23)
Rodentia	*Dipodomys merriami*	752	0.68 (0.02)	0.95 (0.03)
Rodentia	*Dipodomys microps*	121	0.71 (0.06)	0.68 (0.16)
Rodentia	*Dipodomys ordii*	641	0.63 (0.03)	0.91 (0.05)
Rodentia	*Dipodomys simulans*	135	0.73 (0.06)	0.74 (0.21)
Rodentia	*Erethizon dorsatum*	2,522	0.72 (0.01)	0.93 (0.05)
Rodentia	*Geomys breviceps*	102	0.65 (0.04)	0.63 (0.10)
Rodentia	*Geomys bursarius*	361	0.64 (0.04)	0.71 (0.24)
Rodentia	*Geomys pinetis*	109	0.60 (0.06)	0.40 (0.20)
Rodentia	*Glaucomys sabrinus*	441	0.81 (0.03)	0.95 (0.03)
Rodentia	*Glaucomys volans*	720	0.72 (0.02)	0.95 (0.03)
Rodentia	*Heteromys irroratus*	87	0.64 (0.08)	0.56 (0.30)
Rodentia	*Heteromys pictus*	75	0.70 (0.08)	0.69 (0.15)
Rodentia	*Ictidomys mexicanus*	58	0.85 (0.05)	0.95 (0.03)
Rodentia	*Ictidomys tridecemlineatus*	639	0.67 (0.02)	0.85 (0.12)
Rodentia	*Lemmiscus curtatus*	370	0.66 (0.04)	0.84 (0.09)

Rodentia	*Lemmus trimucronatus*	117	0.72 (0.05)	0.83 (0.05)
Rodentia	*Marmota caligata*	398	0.83 (0.03)	0.97 (0.02)
Rodentia	*Marmota flaviventris*	844	0.80 (0.01)	0.98 (0.01)
Rodentia	*Marmota monax*	2,886	0.78 (0.01)	0.99 (0.00)
Rodentia	*Microdipodops megacephalus*	60	0.68 (0.07)	0.62 (0.18)
Rodentia	*Microtus californicus*	288	0.74 (0.03)	0.90 (0.06)
Rodentia	*Microtus longicaudus*	686	0.81 (0.02)	0.96 (0.02)
Rodentia	*Microtus mexicanus*	83	0.88 (0.03)	0.91 (0.05)
Rodentia	*Microtus miurus*	95	0.76 (0.05)	0.77 (0.07)
Rodentia	*Microtus montanus*	459	0.73 (0.03)	0.93 (0.05)
Rodentia	*Microtus ochrogaster*	245	0.69 (0.03)	0.79 (0.07)
Rodentia	*Microtus oregoni*	59	0.61 (0.09)	0.41 (0.21)
Rodentia	*Microtus pennsylvanicus*	1,900	0.71 (0.01)	0.96 (0.02)
Rodentia	*Microtus pinetorum*	183	0.64 (0.03)	0.72 (0.09)
Rodentia	*Napaeozapus insignis*	233	0.68 (0.03)	0.87 (0.06)
Rodentia	*Neotamias amoenus*	311	0.76 (0.02)	0.88 (0.06)
Rodentia	*Neotamias dorsalis*	185	0.74 (0.02)	0.85 (0.06)
Rodentia	*Neotamias merriami*	119	0.79 (0.04)	0.80 (0.12)
Rodentia	*Neotamias minimus*	616	0.81 (0.02)	0.97 (0.01)
Rodentia	*Neotamias speciosus*	76	0.78 (0.03)	0.85 (0.06)
Rodentia	*Neotamias townsendii*	209	0.67 (0.06)	0.71 (0.17)
Rodentia	*Neotamias umbrinus*	83	0.77 (0.08)	0.83 (0.12)

Rodentia	*Neotoma albigula*	362	0.66 (0.02)	0.68 (0.27)
Rodentia	*Neotoma bryanti*	144	0.70 (0.07)	0.71 (0.17)
Rodentia	*Neotoma cinerea*	341	0.70 (0.02)	0.87 (0.06)
Rodentia	*Neotoma floridana*	224	0.64 (0.05)	0.64 (0.11)
Rodentia	*Neotoma fuscipes*	143	0.71 (0.04)	0.78 (0.09)
Rodentia	*Neotoma lepida*	385	0.61 (0.03)	0.79 (0.07)
Rodentia	*Neotoma leucodon*	110	0.66 (0.06)	0.61 (0.22)
Rodentia	*Neotoma macrotis*	163	0.70 (0.03)	0.77 (0.14)
Rodentia	*Neotoma mexicana*	326	0.76 (0.04)	0.93 (0.04)
Rodentia	*Ochrotomys nuttalli*	102	0.67 (0.06)	0.71 (0.14)
Rodentia	*Onychomys arenicola*	78	0.61 (0.08)	0.42 (0.32)
Rodentia	*Onychomys leucogaster*	691	0.64 (0.01)	0.94 (0.05)
Rodentia	*Onychomys torridus*	167	0.71 (0.04)	0.75 (0.14)
Rodentia	*Osgoodomys banderanus*	51	0.78 (0.05)	0.83 (0.13)
Rodentia	*Otospermophilus beecheyi*	1,082	0.72 (0.03)	0.97 (0.02)
Rodentia	*Otospermophilus variegatus*	1,319	0.78 (0.03)	0.98 (0.01)
Rodentia	*Perognathus fasciatus*	250	0.66 (0.03)	0.74 (0.14)
Rodentia	*Perognathus flavus*	292	0.63 (0.04)	0.75 (0.17)
Rodentia	*Perognathus longimembris*	196	0.66 (0.03)	0.77 (0.08)
Rodentia	*Peromyscus attwateri*	91	0.61 (0.04)	0.58 (0.18)
Rodentia	*Peromyscus boylii*	619	0.72 (0.02)	0.97 (0.02)
Rodentia	*Peromyscus californicus*	114	0.77 (0.03)	0.83 (0.07)

Rodentia	*Peromyscus crinitus*	279	0.62 (0.03)	0.50 (0.23)
Rodentia	*Peromyscus difficilis*	170	0.71 (0.02)	0.81 (0.06)
Rodentia	*Peromyscus eremicus*	454	0.65 (0.03)	0.76 (0.16)
Rodentia	*Peromyscus gossypinus*	147	0.65 (0.09)	0.64 (0.36)
Rodentia	*Peromyscus gratus*	133	0.68 (0.04)	0.68 (0.14)
Rodentia	*Peromyscus keeni*	202	0.77 (0.03)	0.81 (0.07)
Rodentia	*Peromyscus leucopus*	1,757	0.63 (0.03)	0.96 (0.02)
Rodentia	*Peromyscus maniculatus*	3,693	0.65 (0.01)	0.98 (0.01)
Rodentia	*Peromyscus melanophrys*	106	0.62 (0.06)	0.51 (0.27)
Rodentia	*Peromyscus melanotis*	86	0.89 (0.03)	0.92 (0.06)
Rodentia	*Peromyscus nasutus*	94	0.67 (0.07)	0.71 (0.08)
Rodentia	*Peromyscus truei*	596	0.68 (0.02)	0.92 (0.03)
Rodentia	*Poliocitellus franklinii*	96	0.65 (0.08)	0.60 (0.25)
Rodentia	*Reithrodontomys fulvescens*	367	0.61 (0.03)	0.74 (0.11)
Rodentia	*Reithrodontomys humulis*	55	0.61 (0.09)	0.44 (0.29)
Rodentia	*Reithrodontomys megalotis*	930	0.69 (0.02)	0.96 (0.02)
Rodentia	*Reithrodontomys sumichrasti*	113	0.83 (0.03)	0.82 (0.10)
Rodentia	*Sciurus aberti*	248	0.86 (0.03)	0.91 (0.06)
Rodentia	*Sciurus aureogaster*	421	0.72 (0.04)	0.89 (0.07)
Rodentia	*Sciurus carolinensis*	5,346	0.78 (0.01)	1.00 (0.00)
Rodentia	*Sciurus griseus*	522	0.80 (0.01)	0.96 (0.03)
Rodentia	*Sciurus nayaritensis*	68	0.73 (0.06)	0.69 (0.12)

Rodentia	*Sciurus niger*	2,800	0.78 (0.02)	1.00 (0.00)
Rodentia	*Sciurus oculatus*	51	0.70 (0.05)	0.69 (0.11)
Rodentia	*Sigmodon arizonae*	67	0.76 (0.06)	0.90 (0.05)
Rodentia	*Sigmodon hispidus*	1,099	0.68 (0.02)	0.96 (0.03)
Rodentia	*Synaptomys borealis*	155	0.78 (0.05)	0.90 (0.03)
Rodentia	*Synaptomys cooperi*	86	0.63 (0.05)	0.64 (0.11)
Rodentia	*Tamias striatus*	4,037	0.71 (0.01)	0.99 (0.00)
Rodentia	*Tamiasciurus douglasii*	730	0.76 (0.02)	0.97 (0.02)
Rodentia	*Tamiasciurus hudsonicus*	4,228	0.76 (0.00)	1.00 (0.00)
Rodentia	*Thomomys bottae*	949	0.80 (0.01)	0.97 (0.02)
Rodentia	*Thomomys talpoides*	441	0.71 (0.03)	0.94 (0.03)
Rodentia	*Thomomys umbrinus*	98	0.74 (0.06)	0.85 (0.06)
Rodentia	*Urocitellus armatus*	154	0.78 (0.04)	0.85 (0.05)
Rodentia	*Urocitellus beldingi*	149	0.84 (0.04)	0.87 (0.04)
Rodentia	*Urocitellus columbianus*	379	0.73 (0.02)	0.90 (0.03)
Rodentia	*Urocitellus elegans*	52	0.78 (0.07)	0.85 (0.07)
Rodentia	*Urocitellus mollis*	67	0.78 (0.08)	0.83 (0.06)
Rodentia	*Urocitellus richardsonii*	378	0.67 (0.02)	0.88 (0.07)
Rodentia	*Xerospermophilus spilosoma*	189	0.69 (0.04)	0.78 (0.12)
Rodentia	*Xerospermophilus tereticaudus*	192	0.81 (0.03)	0.89 (0.03)
Rodentia	*Zapus hudsonius*	612	0.72 (0.02)	0.90 (0.08)
Rodentia	*Zapus princeps*	380	0.79 (0.04)	0.94 (0.06)

Soricomorpha	*Blarina brevicauda*	1,916	0.69 (0.02)	0.98 (0.01)
Soricomorpha	*Blarina carolinensis*	181	0.74 (0.01)	0.82 (0.09)
Soricomorpha	*Blarina hylophaga*	116	0.65 (0.07)	0.66 (0.17)
Soricomorpha	*Condylura cristata*	401	0.73 (0.04)	0.93 (0.04)
Soricomorpha	*Cryptotis parva*	429	0.67 (0.04)	0.77 (0.10)
Soricomorpha	*Neurotrichus gibbsii*	194	0.73 (0.04)	0.86 (0.07)
Soricomorpha	*Notiosorex crawfordi*	145	0.76 (0.04)	0.85 (0.06)
Soricomorpha	*Parascalops breweri*	239	0.66 (0.03)	0.78 (0.11)
Soricomorpha	*Scalopus aquaticus*	571	0.76 (0.03)	0.95 (0.04)
Soricomorpha	*Scapanus latimanus*	213	0.80 (0.04)	0.84 (0.05)
Soricomorpha	*Scapanus orarius*	85	0.74 (0.08)	0.78 (0.12)
Soricomorpha	*Scapanus townsendii*	58	0.77 (0.07)	0.87 (0.12)
Soricomorpha	*Sorex arcticus*	72	0.63 (0.11)	0.56 (0.26)
Soricomorpha	*Sorex cinereus*	1,494	0.72 (0.01)	0.99 (0.01)
Soricomorpha	*Sorex fumeus*	150	0.71 (0.05)	0.76 (0.13)
Soricomorpha	*Sorex haydeni*	140	0.63 (0.05)	0.62 (0.19)
Soricomorpha	*Sorex hoyi*	221	0.69 (0.04)	0.75 (0.12)
Soricomorpha	*Sorex longirostris*	65	0.68 (0.10)	0.72 (0.14)
Soricomorpha	*Sorex monticolus*	952	0.79 (0.01)	0.97 (0.02)
Soricomorpha	*Sorex nanus*	59	0.76 (0.12)	0.88 (0.10)
Soricomorpha	*Sorex ornatus*	99	0.73 (0.07)	0.77 (0.14)
Soricomorpha	*Sorex palustris*	207	0.78 (0.05)	0.89 (0.07)

Soricomorpha	*Sorex trowbridgii*	193	0.72 (0.04)	0.82 (0.10)
Soricomorpha	*Sorex vagrans*	278	0.70 (0.01)	0.89 (0.02)

Table S2. List of anthropogenic factors (A) and climatic variables (C) used in the modeling experiment.

Group	Variable name	Acronym	Original spatial resolution	Temporal extent	Reference
A	Human Impact Index	Human Impact Index	30 arc-second (ca. 1 km)	2010	(Sanderson *et al.* 2022)
	Human Population (people/km^2)	Human population	30 arc-second (ca. 1km)	2010	(Bright *et al.* 2011)
	Cropland (%)	Cropland	5 arc-min (ca. 10 km)	2000	(Ramankutty *et al.* 2010a)
	Pasture (%)	Pasture	5 arc-min (ca. 10 km)	2000	(Ramankutty *et al.* 2010b)
	Annual Nighttime Lights (nW/cm^2/sr)	Nighttime lights	15 arc-second (ca. 500 m)	2012	(Elvidge *et al.* 2021)
	Highway Density (m/km^2)	Highway density	5 arc-minute (ca. 10 km)	2018	(Meijer *et al.* 2018)
C	Annual Mean Temperature (°C)	Annual mean T	30 arc-second (ca. 1km)	1991-2020	(AdaptWest Project 2022)
	Annual Precipitation (mm)	Annual P	30 arc-second (ca. 1km)	1991-2020	
	Mean Temperature of Warmest Quarter (°C)	Maximum T	30 arc-second (ca. 1km)	1991-2020	
	Mean Temperature of Coldest Quarter (°C)	Minimum T	30 arc-second (ca. 1km)	1991-2020	
	Precipitation of Wettest Quarter (mm)	Wettest P	30 arc-second (ca. 1km)	1991-2020	
	Precipitation of Driest Quarter (mm)	Driest P	30 arc-second (ca. 1km)	1991-2020	

nW/cm^2/sr: unit of radiance; nanowatt(s) per steradian per square centimeter.

Table S3. Number of species for which the human impact index (HII) had greater permutation importance than selected climatic variables.

Order	Number of species	HII > Maximum T	HII > Minimum T	HII > Annual mean T	HII > Annual P
Artiodactyla	8	6	7	8	6
Carnivora	18	16	13	13	16
Chiroptera	28	25	21	20	24
Didelphimorphia	1	1	1	1	1
Lagomorpha	13	10	8	11	11
Rodentia	127	85	88	92	103
Soricomorpha	24	15	12	14	20
All species	219	158	150	159	181

Table S4. Biological traits for the focal mammal species.

Group	Trait	Variable name	Definition	Data type	
Size	Body mass	adult_mass_g	Adult body mass in grams	Numeric	Selected
	Brain mass	brain_mass_g	Adult's brain weight, expressed in grams	Numeric	
	Body length	adult_body_length_mm	Total length, measured in millimeters, of an adult individual's nose tip to anus or base of tail	Numeric	
Growth and reproduction	Maximum longevity	max_longevity_d	Maximum age in days recorded at death for the species	Numeric	
	Female sexual maturity	female_maturity_d	The number of days required to reach sexual maturity for a female	Numeric	Selected
	Age of first reproduction	age_first_reproduction_d	The age at which a female gives birth to her first litter or the number of days that her young attach to her teats	Numeric	
	Gestation length	gestation_length_d	Days that a fetus takes to grow	Numeric	Selected
	Litter size	litter_size_n	Number of offspring born to a female in a litter	Numeric	Selected
	Number of litters	litters_per_year_n	Number of litters per female per year	Numeric	Selected
	Time between reproduction events	interbirth_interval_d	Time between reproduction events in days	Numeric	

	Weaning age	weaning_age_d	Age at which an individual's primary dietary dependence on their mother ceases and their ability to forage independently begin	Numeric	Selected
	Generation length	generation_length_d	The current cohort's parents' average age in days	Numeric	Selected
	Hibernation	hibernation_torpor	Members of the species exhibit torpor or hibernation.	Binary	Selected
Diet composition from PHYLACINE v. 1.2	Invertebrates on diet	dphy_invertebrate	Percentage of the diet composed of invertebrates	Numeric	
	Vertebrates on diet	dphy_vertebrate	Percentage of the diet composed of vertebrates	Numeric	
	Plants and/or fungi on diet	dphy_plant	Percentage of the diet composed of plants and/or fungi	Numeric	
Diet composition from EltonTraits	Diet breadth	det_diet_breadth_n	Number of prevalent (≥ 20%) EltonTraits dietary categories Consumed, from 1 to 5	Numeric	Selected
Trophic level	Trophic level	trophic_level	Trophic level os the species: carnivore, omnivore and herbivore	Ordinal. Three levels: herbivore, omnivore and carnivore	Selected
Habitat use	Fossoriality	fossoriality	The species is above ground dwelling or ground/fossorial dwelling	Binary	Selected
	Foraging strata	foraging_stratum	Where the species forage	Ordinal. Five levels:	Selected

				marine, ground, scansorial, arboreal and aerial	
	Activity cycle	activity_cycle	Activity cycle of each species	Ordinal. Three levels: nocturnal only, mixed, and diurnal only	Selected
	Volant capacity	terrestrial_volant	Capacity of powered flight and the species spends a significant amount of time flying in the air	Binary	Selected
	Habitat breadth	habitat_breadth_n	Number of distinct suitable level 1 IUCN habitats	Numeric	Selected

Table S5. Estimated lambdas for the model residuals across 1,000 phylogenetic trees.

Order	Model type	Mean lambda across 1,000 trees
All	StepAIC	0.0000733
	Full	0.0000733
Carnivora	StepAIC	0.0000751
	Full	0.0000751
Chiroptera	StepAIC	0.0000750
	Full	0.0000750
Lagomorpha	StepAIC	0.0000741
	Full	0.0000741
Rodentia	StepAIC	0.0000734
	Full	0.0000734
Soricomorpha	StepAIC	0.0000743
	Full	0.0000743

Table S6. Estimated coefficients for the stepAIC OLS models. P-values indicate the significance of the estimated coefficient different from zero.

Model	*Trait*	*Estimate (95% CI)*	*P-value*
All (N = 219)	*Adult mass (g)*	*0.184 (0.100, 0.268)*	*0.000*
	Ground foraging	*-0.436 (-0.777, -0.095)*	*0.013*
	Arboreal foraging	*-0.212 (-0.528, 0.105)*	*0.189*
	Scansorial foraging	*-0.184 (-0.528, 0.160)*	*0.292*
	Terrestrial volant	*0.604 (0.261, 0.947)*	*0.001*
	Above ground dwelling	*-0.122 (-0.255, 0.010)*	*0.069*
	Gestation length	*-0.109 (-0.173, -0.046)*	*0.001*
	Generation length (days)	*-0.080 (-0.157, -0.002)*	*0.043*
Carnivora (N = 18)	*Adult mass (g)*	*-0.187 (-0.380, 0.006)*	*0.057*
	Noctural/diurnal/crepuscular	*0.256 (-0.012, 0.524)*	*0.060*
Chiroptera (N = 28)	*Diet breadth*	*-0.180 (-0.338, -0.021)*	*0.028*
	Litter size	*0.219 (-0.009, 0.448)*	*0.059*
	Female maturity (days)	*0.157 (-0.045, 0.359)*	*0.121*
	Weaning age (days)	*0.129 (-0.034, 0.291)*	*0.116*
Lagomorpha (N = 13)	*Adult mass (g)*	*0.671 (0.234, 1.108)*	*0.007*
	Gestation length	*-1.351 (-2.791, 0.089)*	*0.063*
Rodentia (N = 127)	*Above ground dwelling*	*-0.215 (-0.356, -0.073)*	*0.003*
	Habitat breadth	*0.064 (-0.014, 0.141)*	*0.107*
	Weaning age (days)	*0.246 (0.116, 0.377)*	*0.000*
Soricomorpha (N = 24)	*Adult mass (g)*	*1.404 (0.824, 1.984)*	*0.000*
	Carnivory	*-0.188 (-0.540, 0.165)*	*0.273*
	Diet breadth	*0.343 (0.003, 0.683)*	*0.048*
	Noctural/diurnal/crepuscular	*-1.230 (-2.137, -0.323)*	*0.011*
	Habitat breadth	*0.118 (-0.051, 0.286)*	*0.156*
	Litters per year	*-0.690 (-1.220, -0.159)*	*0.014*
	Litter size	*0.293 (0.019, 0.567)*	*0.038*

	Gestation length	*-1.985 (-3.480, -0.491)*	*0.013*
	Weaning age (days)	*-0.511 (-1.299, 0.277)*	*0.186*